Generative Models II: Explicit Density Models

AI602: Recent Advances in Deep Learning

Lecture 5

Slide made by

Sangwoo Mo and Chaewon Kim

KAIST EE

Table of Contents

Table of Contents

Implicit vs Explicit Density Models

- From now on, we study generative models with explicit density estimation:

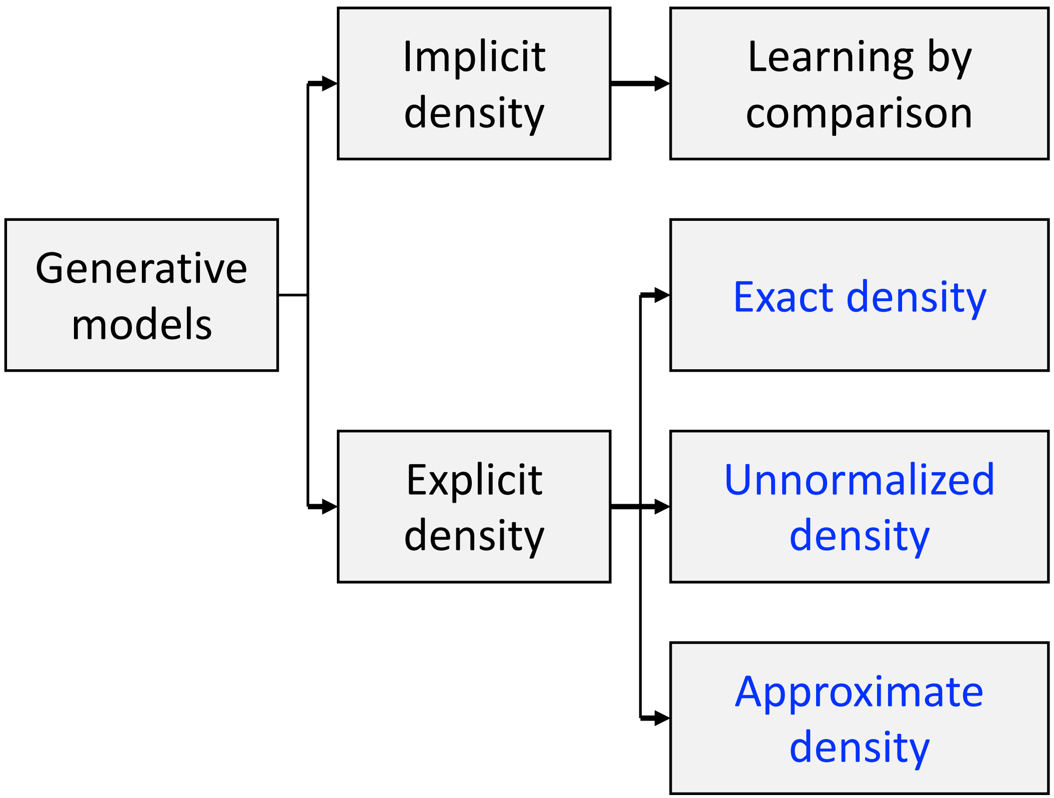

- Only care about generation, not $p(x)$
- Instead of maximizing density, compare real vs generated samples (i.e., reduce generation problem to classification)
- Example: GAN, GMMN

- Directly learn density $p(x)$
- Example: autoregressive, flow

- Learn unnormalized density $E(x) \propto p(x)$
- Example: EBM, score matching

- Learn approximation (e.g., lower bound) of density $\mathcal{L}(x) \leq p(x)$
- Example: VAE, diffusion model

- From now on, we study generative models with explicit density estimation:

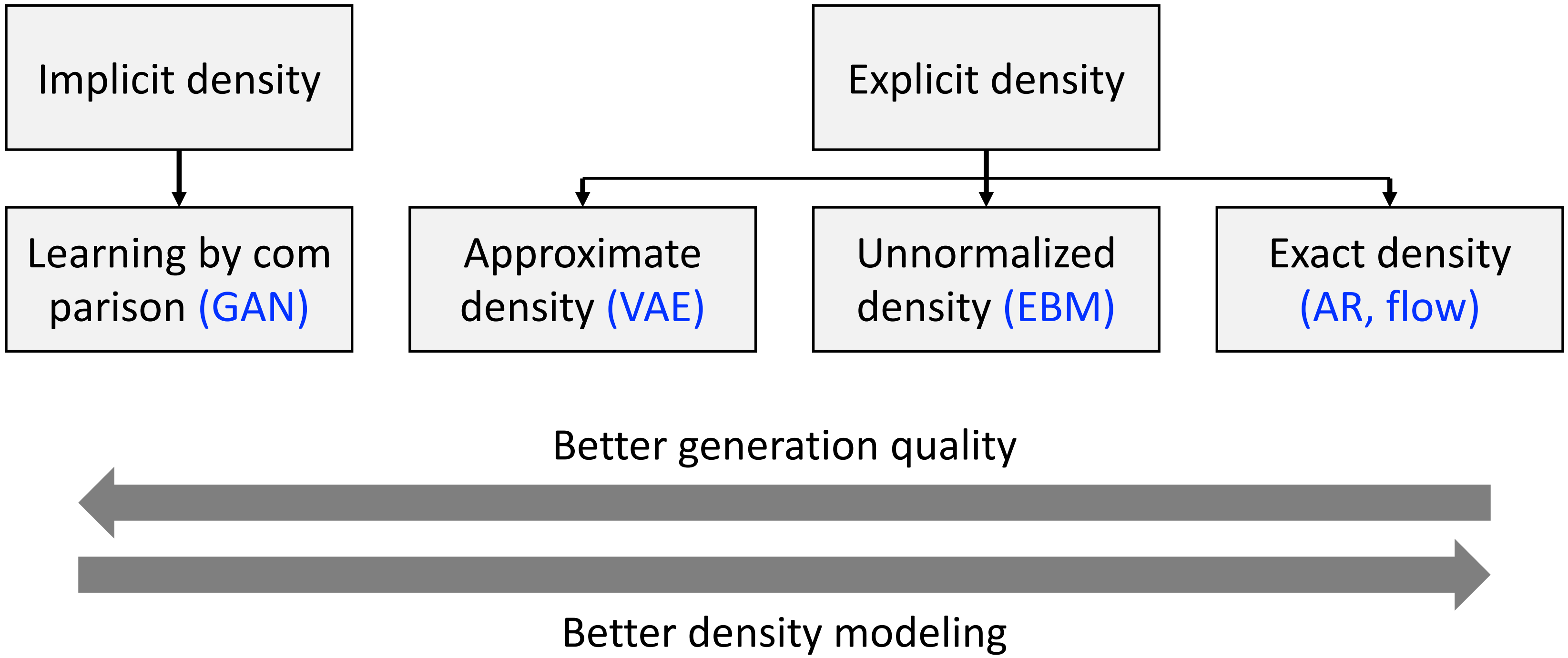

Table of Contents

- Consider the following generative model:

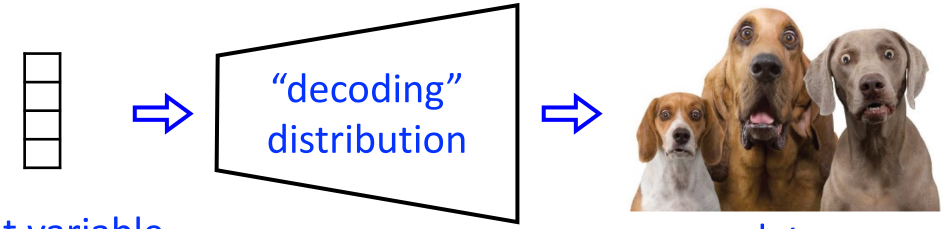

latent variable $\boldsymbol{z}$

data $\boldsymbol{x}$

  - Fixed prior on random latent variable
    - e.g., standard Normal distribution

$$p(\boldsymbol{z}) = \mathcal{N}(\boldsymbol{z}; \mathbf{0}, \mathbb{I})$$

  - Parameterized likelihood (decoder) for generation:
    - e.g., Normal distribution parameterized by neural network

$$p_\theta(\boldsymbol{x}|\boldsymbol{z}) = \mathcal{N}(\boldsymbol{x}; f_{\texttt{dec}}(\boldsymbol{z}), \mathbb{I})$$

  - Resulting generative distribution (to optimize):

$$\log p_\theta(\boldsymbol{x}) = \log \int_{\boldsymbol{z}} p_\theta(\boldsymbol{x}|\boldsymbol{z}) p(\boldsymbol{z}) d\boldsymbol{z} = \log \mathbb{E}_{\boldsymbol{z}\sim p(\boldsymbol{z})}[p(\boldsymbol{x}|\boldsymbol{z})]$$

Variational Autoencoder (VAE)

- Variational autoencoder (VAE) introduce an auxiliary distribution (encoder) [Kingma et al., 2013]

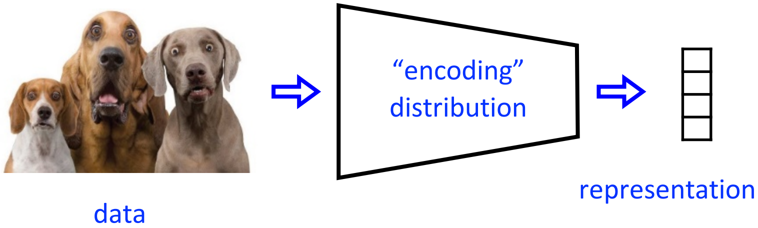

$$q_\phi(\boldsymbol{z}|\boldsymbol{x}) = \mathcal{N}(\boldsymbol{z}; f_{\texttt{enc},\mu}(\boldsymbol{x}), f_{\texttt{enc},\sigma}(\boldsymbol{x}))$$

- Each $\log p_\theta(\boldsymbol{x})$ term is replaced by its lower bound:

$$\begin{aligned}
\log p_\theta(\boldsymbol{x}) &\geq \log p_\theta(\boldsymbol{x}) - \min_\phi \mathrm{KL}(q_\phi(\boldsymbol{z}|\boldsymbol{x})||p_\theta(\boldsymbol{z}|\boldsymbol{x})) \\
&= \log p_\theta(\boldsymbol{x}) + \max_\phi \mathbb{E}_{\boldsymbol{z}\sim q_\phi(\boldsymbol{z}|\boldsymbol{x})}[\log p_\theta(\boldsymbol{z}|\boldsymbol{x}) - \log q_\phi(\boldsymbol{z}|\boldsymbol{x})] \\
&= \max_\phi \mathbb{E}_{\boldsymbol{z}\sim q_\phi(\boldsymbol{z}|\boldsymbol{x})}[\log p_\theta(\boldsymbol{x}) + \log p_\theta(\boldsymbol{z}|\boldsymbol{x}) - \log q_\phi(\boldsymbol{z}|\boldsymbol{x})] \\
&= \max_\phi \mathbb{E}_{\boldsymbol{z}\sim q_\phi(\boldsymbol{z}|\boldsymbol{x})}[\log p_\theta(\boldsymbol{x}|\boldsymbol{z})] - \mathrm{KL}(q_\phi(\boldsymbol{z}|\boldsymbol{x})||p(\boldsymbol{z}))
\end{aligned}$$

- Bound becomes equality when $q_\phi(\boldsymbol{z}|\boldsymbol{x}) \approx p_\theta(\boldsymbol{z}|\boldsymbol{x})$

- The training objective becomes:

tractable between two Gaussian distributions

$$\max_{\theta} \sum_{n=1}^{N} \log p_\theta(\boldsymbol{x}^{(n)}) \geq \max_{\theta} \max_{\phi} \mathbb{E}_{\boldsymbol{z}\sim q_\phi(\boldsymbol{z}|\boldsymbol{x})}[\log p_\theta(\boldsymbol{x}|\boldsymbol{z})] - \mathrm{KL}(q_\phi(\boldsymbol{z}|\boldsymbol{x})||p(\boldsymbol{z}))$$

$$\approx \max_{\theta} \max_{\phi} \sum_{n=1}^{N} \sum_{k=1}^{N} \log p_\theta(\boldsymbol{x}^{(n)}|\boldsymbol{z}^{(n,k)}) - \mathrm{KL}(q_\phi(\boldsymbol{z}|\boldsymbol{x}^{(n)})||p(\boldsymbol{z}))$$

where latent variables are sampled by $\boldsymbol{z}^{(n,k)} \sim q_\phi(\boldsymbol{z}|\boldsymbol{x}^{(n)})$

- However, non-trivial to train with back propagation due to sampling procedure:

$$\nabla_\phi \mathcal{L} = \sum_{n=1}^{N} \sum_{k=1}^{N} - \nabla_\phi \log p_\theta(\boldsymbol{x}^{(n)}|\boldsymbol{z}^{(n,k)}) + \nabla_\phi \mathrm{KL}(q_\phi(\boldsymbol{z}|\boldsymbol{x}^{(n)})||p(\boldsymbol{z}))$$

$\Downarrow$

Since $\boldsymbol{z}^{(n,k)}$ is fixed after being sampled, $\nabla_\phi \log p(\boldsymbol{x}^{(n)}|\boldsymbol{z}^{(n,k)}) = 0$?

- Reparameterization trick is based on the change-of-variables formula:

$$\varepsilon_2 \sim \mathcal{N}(\varepsilon_2|\mu,\sigma) \Leftrightarrow \varepsilon_2 = \mu + \sigma\varepsilon_0, \qquad \varepsilon_0 \sim \mathcal{N}(\varepsilon_0|0,1)$$

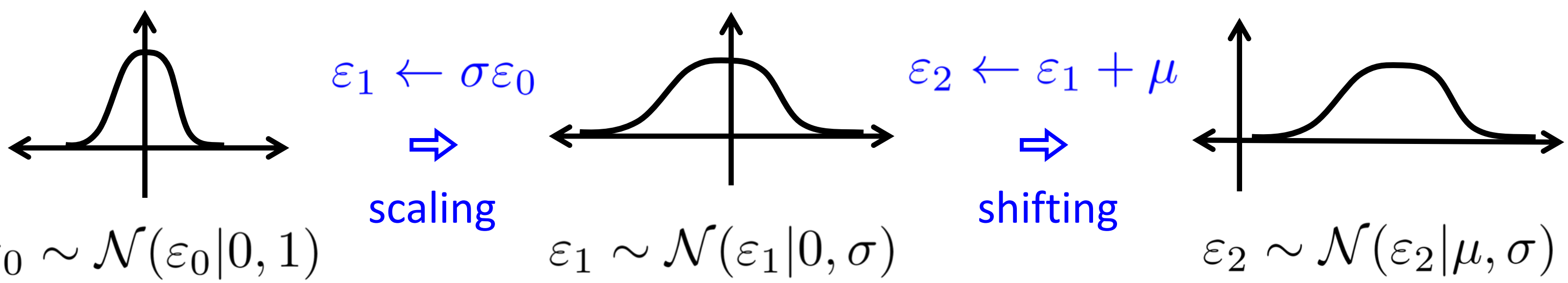

- Latent variable $\boldsymbol{z}^{(n,k)}$ can be similarly parameterized by encoder network:

$$\boldsymbol{z}^{(n,k)} \sim \mathcal{N}(\boldsymbol{z}; f_{\texttt{enc},\mu}(\boldsymbol{x}^{(n)}), f_{\texttt{enc},\sigma}(\boldsymbol{x}^{(n)}))$$

$$\Updownarrow$$

$$\boldsymbol{z}^{(n,k)} = f_{\texttt{enc},\mu}(\boldsymbol{x}^{(n)}) + f_{\texttt{enc},\sigma}(\boldsymbol{x}^{(n)}) \odot \boldsymbol{\varepsilon}^{(n,k)}, \qquad \boldsymbol{\varepsilon}^{(n,k)} \sim \mathcal{N}(\boldsymbol{\varepsilon}|\mathbf{0},\mathbf{1})$$

- Total loss of variational autoencoder:

$$\nabla_\phi \mathcal{L} = \sum_{n=1}^{N} \sum_{k=1}^{N} \underbrace{- \nabla_\phi \log p_\theta(\boldsymbol{x}^{(n)} | \boldsymbol{z}^{(n,k)})}_{\nabla_\phi \mathcal{L}_1} + \underbrace{\nabla_\phi \mathrm{KL}(q_\phi(\boldsymbol{z}|\boldsymbol{x}^{(n)}) || p(\boldsymbol{z}))}_{\nabla_\phi \mathcal{L}_2}$$

- Recall that $f_{\texttt{dec}}, f_{\texttt{enc},\mu}, f_{\texttt{enc},\sigma}$ are parameterized by ϕ

- Derivative of first part:

$$\nabla_\phi \mathcal{L}_1 = \nabla_\phi \log \mathcal{N}(\boldsymbol{x}^{(n)}; f_{\texttt{dec}}(\boldsymbol{z}^{(n,k)}), \mathbf{1})$$

$\Downarrow$ log-normal distribution

$$= \nabla_\phi \frac{1}{2} \| \boldsymbol{x}^{(n)} - f_{\texttt{dec}}(\boldsymbol{z}^{(n,k)}) \|_2^2$$

$\Downarrow$ reparameterization trick

$$= \nabla_\phi \frac{1}{2} \| \boldsymbol{x}^{(n)} - f_{\texttt{dec}}(f_{\texttt{enc},\mu}(\boldsymbol{x}^{(n)}) + f_{\texttt{enc},\sigma}(\boldsymbol{x}^{(n)}) \odot \boldsymbol{\varepsilon}^{(n,k)}) \|_2^2$$

- Total loss of variational autoencoder:

$$\nabla_\phi \mathcal{L} = \sum_{n=1}^{N} \sum_{k=1}^{N} - \underbrace{\nabla_\phi \log p_\theta(\boldsymbol{x}^{(n)} | \boldsymbol{z}^{(n,k)})}_{\nabla_\phi \mathcal{L}_1} + \underbrace{\nabla_\phi \mathrm{KL}(q_\phi(\boldsymbol{z}|\boldsymbol{x}^{(n)}) || p(\boldsymbol{z}))}_{\nabla_\phi \mathcal{L}_2}$$

- Recall that $f_{\texttt{dec}}, f_{\texttt{enc},\mu}, f_{\texttt{enc},\sigma}$ are parameterized by ϕ

- Derivative of second part:

$$\nabla_\phi \mathcal{L}_1 = \nabla_\phi \mathrm{KL}(\mathcal{N}(\boldsymbol{z}; f_{\texttt{enc},\mu}(\boldsymbol{x}^{(n)}), f_{\texttt{enc},\sigma}(\boldsymbol{x}^{(n)})) || \mathcal{N}(\boldsymbol{z}; \mathbf{0}, \mathbf{1}))$$

$\Downarrow$ element-wise factorization ($\boldsymbol{z} = [z_1, \cdots, z_K]$)

$$= \sum_{k=1}^{K} \nabla_\phi \mathrm{KL}(\mathcal{N}(z_k; f_{\texttt{enc},\mu,k}(\boldsymbol{x}^{(n)}), f_{\texttt{enc},\sigma,k}(\boldsymbol{x}^{(n)})) || \mathcal{N}(z_k; 0, 1))$$

$\Downarrow$ KL divergence between normal distributions

$$= \sum_{k=1}^{K} \nabla_\phi - \log f_{\texttt{enc},\sigma,k}(\boldsymbol{x}^{(n)}) + \frac{1}{2} f_{\texttt{enc},\sigma,k}(\boldsymbol{x}^{(n)})^2 + \frac{1}{2} f_{\texttt{enc},\sigma,k}(\boldsymbol{x}^{(n)})^2$$

Variational Autoencoder (VAE)

- Based on the proposed scheme, variational autoencoder successfully generates images:

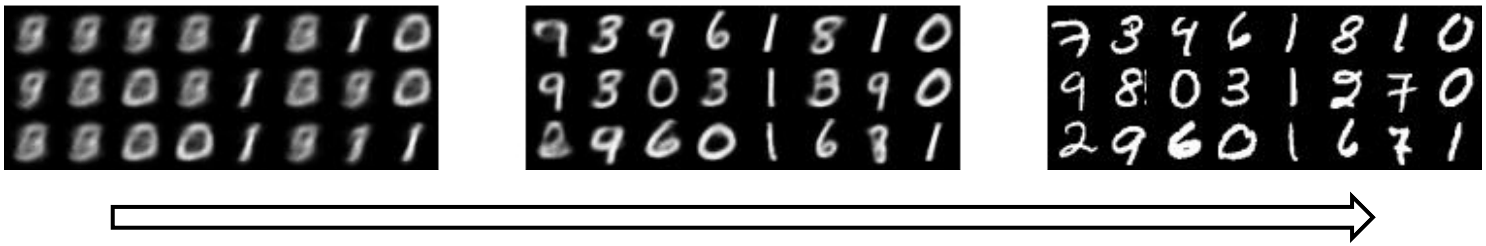

Training on MNIST

- Interpolation of latent variables induce transitions in generated images:

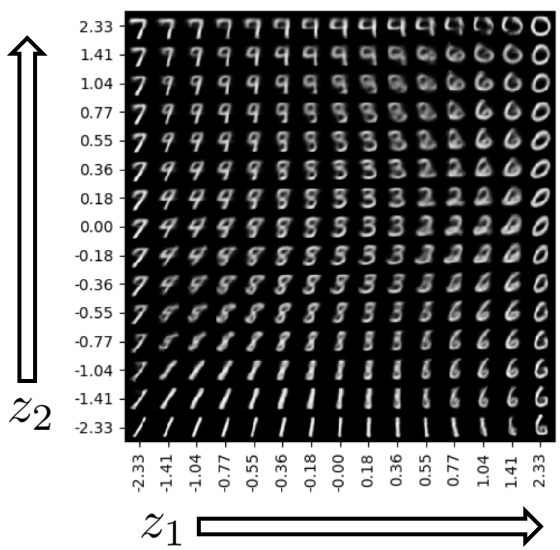

- Although VAE has many advantages (e.g., fast sampling, full mode covering, latent embedding), there are issues that lead to **poor generation quality**

- Tighter objective bound
  - **Reduce approximation (model) error:** Importance-weighted AE (IWAE)
  - **Reduce amortization (sample-wise) error:** Semi-amortized VAE (SA-VAE)

- Posterior collapse (latents are ignored when paired with powerful decoder)
  - **Careful optimization:** various techniques for continuous latent-space VAEs
  - **Use discrete latent space:** Vector-quantized VAE (VQ-VAE)

- Improve model expressivity
  - **Use expressive prior distribution:** Gaussian mixtures, normalizing flow
  - **Use hierarchical architectures:** Hierarchical VAE, Diffusion Models

- Although VAE has many advantages (e.g., fast sampling, full mode covering, latent embedding), there are issues that lead to **poor generation quality**

- Tighter objective bound
  - **Reduce approximation (model) error:** Importance-weighted AE (IWAE)
  - **Reduce amortization (sample-wise) error:** Semi-amortized VAE (SA-VAE)

- Posterior collapse (latents are ignored when paired with powerful decoder)
  - **Careful optimization:** various techniques for continuous latent-space VAEs
  - **Use discrete latent space:** Vector-quantized VAE (VQ-VAE)

- Improve model expressivity
  - **Use expressive prior distribution:** Gaussian mixtures, normalizing flow
  - **Use hierarchical architectures:** Hierarchical VAE, Diffusion Models

- Observe that ELBO can also be proved by the Jensen's inequality:

$$\log p(\boldsymbol{x}) = \log \mathbb{E}_{\boldsymbol{z}\sim q_\phi(\boldsymbol{z}|\boldsymbol{x})}\left[\frac{p(\boldsymbol{x},\boldsymbol{z})}{q_\phi(\boldsymbol{z}|\boldsymbol{x})}\right] \geq \mathbb{E}_{\boldsymbol{z}\sim q_\phi(\boldsymbol{z}|\boldsymbol{x})}\left[\log \frac{p(\boldsymbol{x},\boldsymbol{z})}{q_\phi(\boldsymbol{z}|\boldsymbol{x})}\right]$$

  - Based on convexity, interchange order of logarithm and summation

- Importance weighted AE (IWAE) relax the inequality [Burda et al., 2018]:

$$\log p(\boldsymbol{x}) = \log \mathbb{E}_{\boldsymbol{z}^{(1)},\cdots,\boldsymbol{z}^{(K)}\sim q_\phi(\boldsymbol{z}|\boldsymbol{x})}\left[\frac{1}{K}\sum_{k=1}^{K}\frac{p(\boldsymbol{x},\boldsymbol{z}^{(k)})}{q_\phi(\boldsymbol{z}^{(k)}|\boldsymbol{x})}\right]$$

$$\geq \mathbb{E}_{\boldsymbol{z}^{(1)},\cdots,\boldsymbol{z}^{(K)}\sim q_\phi(\boldsymbol{z}|\boldsymbol{x})}\left[\log \frac{1}{K}\sum_{k=1}^{K}\boxed{\frac{p(\boldsymbol{x},\boldsymbol{z}^{(k)})}{q_\phi(\boldsymbol{z}^{(k)}|\boldsymbol{x})}}\right]$$

also called importance weights

  - Becomes original ELBO when $K=1$ and becomes exact bound when $K=\infty$

$$\mathbb{E}_{\boldsymbol{z}^{(1)},\cdots,\boldsymbol{z}^{(K)}\sim q_\phi(\boldsymbol{z}|\boldsymbol{x})}\left[\frac{1}{K}\sum_{k=1}^{K}\frac{p(\boldsymbol{x},\boldsymbol{z}^{(k)})}{q_\phi(\boldsymbol{z}^{(k)}|\boldsymbol{x})}\right] \approx p(\boldsymbol{x})$$

Semi-amortized VAE (SA-VAE)

- Inference gap of VAE can be decomposed to approximation gap (model error) and amortization gap (single neural network amortizes all posteriors)

- Semi-amortized VAE: In addition to the global inference network, update the posterior of each local instance for a few steps [Kim et al., 2018]
  - Resembles MAML (see future lecture)

1. Sample $\mathbf{x} \sim p_{\mathcal{D}}(\mathbf{x})$
2. Set $\lambda_0 = \text{enc}(\mathbf{x}; \phi)$

   → shared to all samples
3. For $k = 0, \ldots, K-1$, set
   $\lambda_{k+1} = \lambda_k + \alpha \nabla_\lambda \text{ELBO}(\lambda_k, \theta, \mathbf{x})$

   → specific to each sample x

- Semi-amortized VAE can further reduce ELBO, applied on top of any VAEs

MODEL	ORACLE GEN	LEARNED GEN
VAE	≤ 21.77	≤ 27.06
SVI	≤ 22.33	≤ 25.82
SA-VAE	≤ 20.13	≤ 25.21
TRUE NLL (EST)	19.63	–

* SVI: Instance-specific posterior only, without amortization

- Although VAE has many advantages (e.g., fast sampling, full mode covering, latent embedding), there are issues that lead to **poor generation quality**

- Tighter objective bound
  - **Reduce approximation (model) error:** Importance-weighted AE (IWAE)
  - **Reduce amortization (sample-wise) error:** Semi-amortized VAE (SA-VAE)

- Posterior collapse (latents are ignored when paired with powerful decoder)
  - **Careful optimization:** various techniques for continuous latent-space VAEs
  - **Use discrete latent space:** Vector-quantized VAE (VQ-VAE)

- Improve model expressivity
  - **Use expressive prior distribution:** Gaussian mixtures, normalizing flow
  - **Use hierarchical architectures:** Hierarchical VAE, Diffusion Models

Mitigating Posterior Collapse for Continuous Latent-space VAEs

- Posterior collapse [Bowman et al., 2016]:
  - When paired with powerful decoder, VAEs often ignore the posterior $q_\phi(z|x)$ and generates generic samples (i.e., reconstruction loss does not decrease well)

- To mitigate posterior collapse, prior works attempt

  1. Weaken the KL regularization term [Bowman et al., 2016, Razavi et al., 2019a]
     - Recall: KL regularization term minimizes $\mathrm{KL}(p_\phi(z|x), p(z))$
     - Anneal the weight during training, or constraint $\geq \delta$

  2. Match aggregated posterior instead of individuals [Tolstikhin et al., 2018]
     - Instead of matching $p_\phi(z|x) \approx p(z)$ for all x, match the aggregated posterior $\mathbb{E}_{x \sim p(x)}\, p_\phi(z|x) \approx p(z)$ (each $p_\phi(z|x)$ is now a deterministic, single point)
     - Need implicit distribution matching techniques (e.g., GAN)

  3. Improve optimization procedure [He et al., 2019]
     - Strengthen the encoder: update encoder until converge, and decoder once

Vector-quantized VAE (VQ-VAE)

- VQ-VAE [Oord et al., 2017]
  - Each data is embedded into combination of 'discrete' latent vectors: $\{e_1, \cdots, e_K\}$
  - **i.e.)** each encoder output is quantized to the nearest vector among K codebook vectors

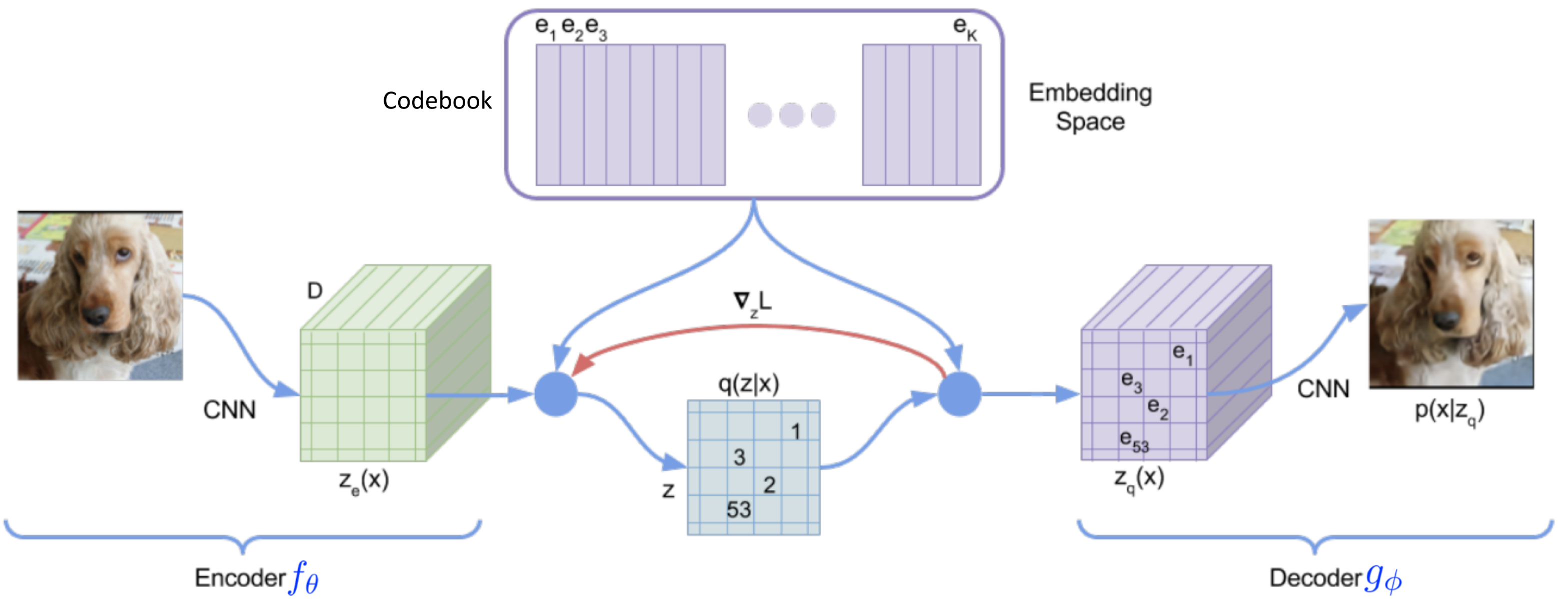

- Restriction of latent space achieves high generation quality including:
  - Images, videos, audios, etc.

Vector-quantized VAE (VQ-VAE)

- VQ-VAE [Oord et al., 2017]
  - The objective of VQ-VAE composed of three terms:
    - Reconstruction loss (1)
    - VQ loss (2):
      - Optimization of codebook vectors
    - Commitment loss (3):
      - Regularization to get encoder outputs and codebook close

$$\mathcal{L} = \underbrace{||g_\phi(e) - x||_2^2}_{(1)} + \underbrace{||\mathbf{sg}(f_\theta(x)) - e||_2^2}_{(2)} + \underbrace{\beta||f_\theta(x) - \mathbf{sg}(e)||_2^2}_{(3)}$$

- VQ-VAE like methods (i.e. discrete prior) recently shows remarkable success on:
  - DALL-E (text-image generative model) – image is encoded via VQ-VAE
  - Many audio self-supervised learning method

- VQ-VAE-2 [Razavi et al., 2019b]
    - Different from VQ-VAE, vector quantization occurs twice (top, bottom level)
    - For both consideration of local/global features for high-fidelity image

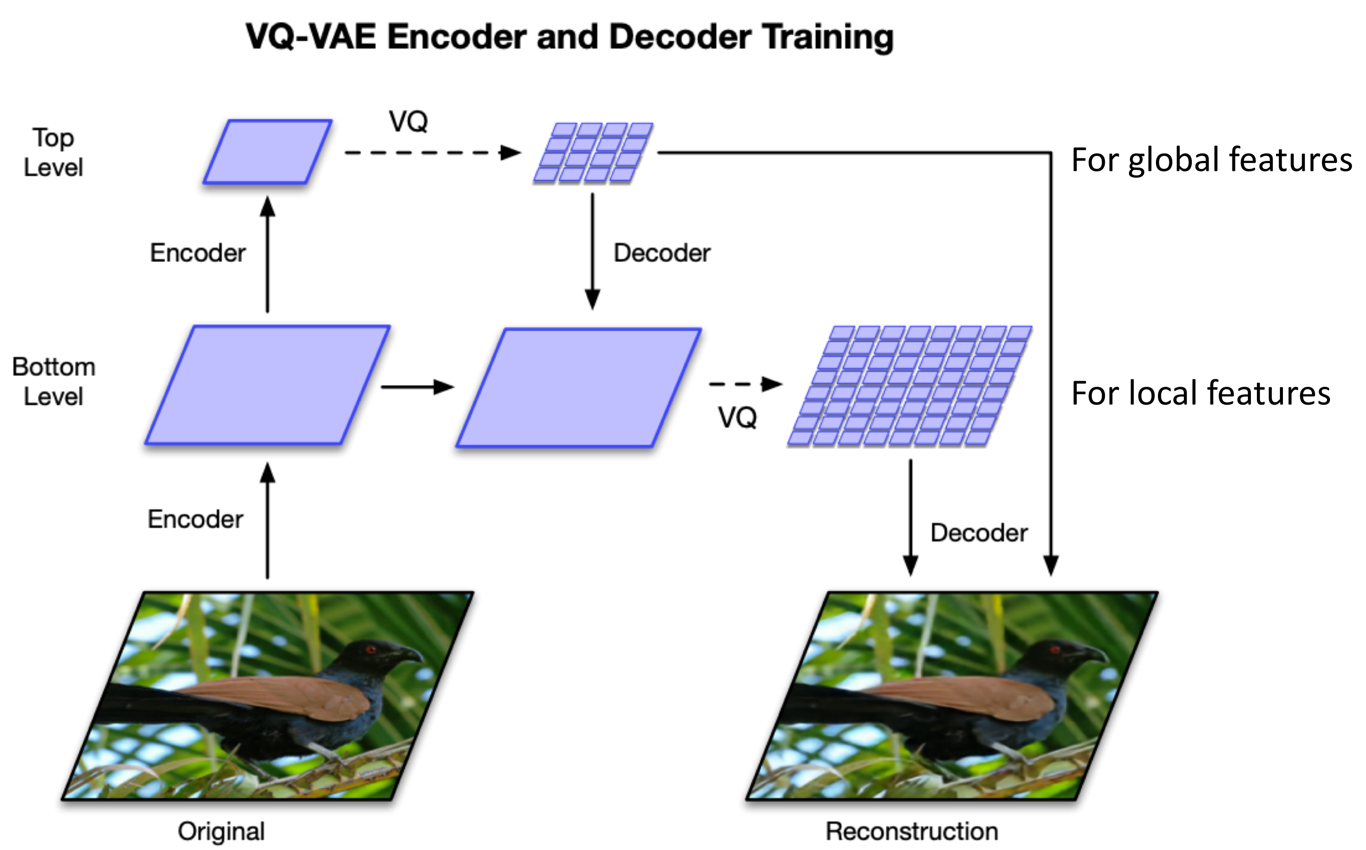

Vector-quantized VAE + Hierarchical Architecture (VQ-VAE-2)

- VQ-VAE-2 [Razavi et al., 2019b]
  - After VQ-VAE-2 training, train two pixelCNN priors for new image generation
  - They autoregressively fill out each quantized latent vector space

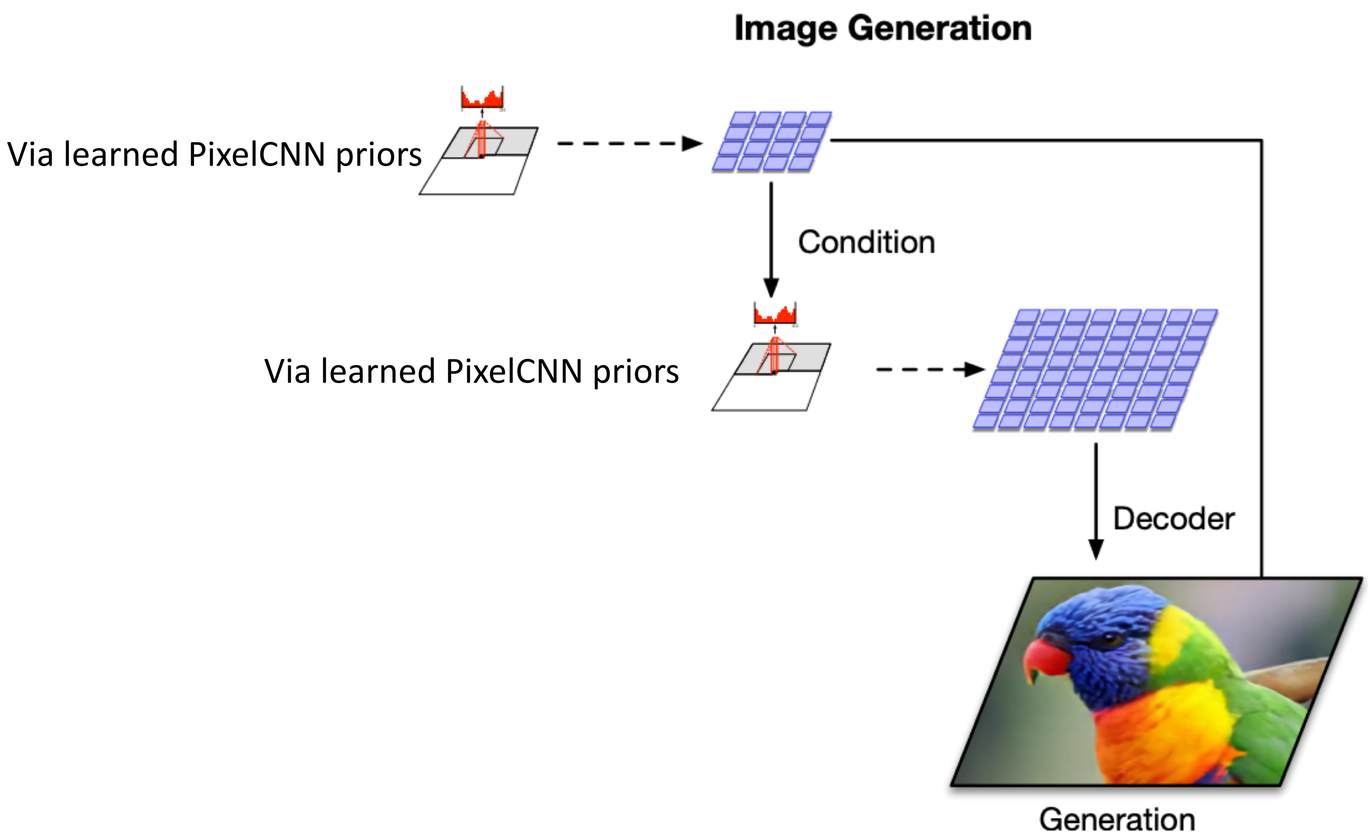

- Generated images are comparable to state-of-the-art GAN model (e.g. BigGAN)

Improving VAEs

- Although VAE has many advantages (e.g., fast sampling, full mode covering, latent embedding), there are issues that lead to **poor generation quality**

- Tighter objective bound
    - **Reduce approximation (model) error:** Importance-weighted AE (IWAE)
    - **Reduce amortization (sample-wise) error:** Semi-amortized VAE (SA-VAE)

- Posterior collapse (latents are ignored when paired with powerful decoder)
    - **Careful optimization:** various techniques for continuous latent-space VAEs
    - **Use discrete latent space:** Vector-quantized VAE (VQ-VAE)

- Improve model expressivity
    - **Use expressive prior distribution:** Gaussian mixtures, normalizing flow
    - **Use hierarchical architectures:** Hierarchical VAE, Diffusion Models

- NVAE [Vahdat et al., 2020]
    - Hierarchical VAEs use the factorized latent space $p_\theta(z) = \prod_l p_\theta(z_l|z_{<l})$
    - Here, the ELBO objective is given by

$$\mathcal{L}_{\mathrm{VAE}}(\boldsymbol{x}) := \mathbb{E}_{q(\boldsymbol{z}|\boldsymbol{x})}\left[\log p(\boldsymbol{x}|\boldsymbol{z})\right] - \mathrm{KL}(q(\boldsymbol{z}_1|\boldsymbol{x})||p(\boldsymbol{z}_1)) - \sum_{l=2}^{L} \mathbb{E}_{q(\boldsymbol{z}_{<l}|\boldsymbol{x})}\left[\mathrm{KL}(q(\boldsymbol{z}_l|\boldsymbol{x}, \boldsymbol{z}_{<l})||p(\boldsymbol{z}_l|\boldsymbol{z}_{<l}))\right],$$

    - However, **prior attempts** on hierarchical VAE were not so successful due to:
        1. Long-range correlation: upper latents often **forget** the data information

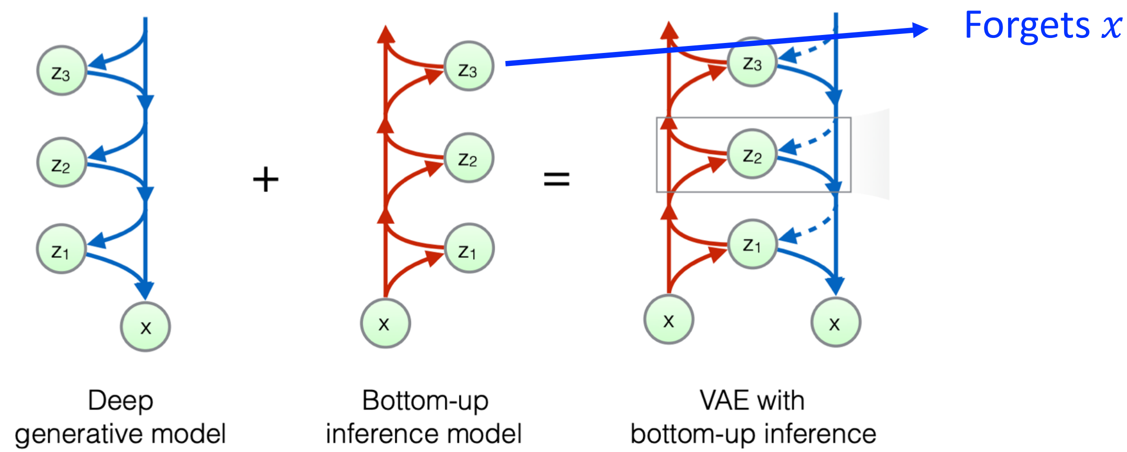

        2. Unstable (unbounded) KL term: even more severe for hierarchical VAEs since they **jointly learn** the prior distribution $p_\theta(z)$

Both $q_\phi(z|x)$ and $p_\theta(z)$ are moving during training

- NVAE [Vahdat et al., 2020]
  - **Idea 1.** Bidirectional encoder (originally from [Kingma et al., 2016])
    - Enforce upper latents (e.g., z_3) to predict the lower latents (e.g., z_1)
      → Improve the long-range correlation issue

Better remembers x
(should reconstruct z_1)

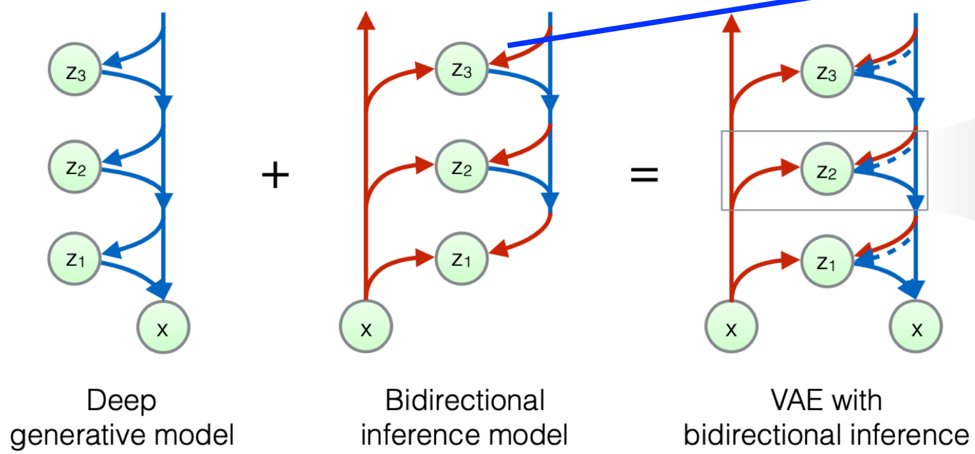

- **Training: posterior** $q_\phi(z|x)$ is inferred by both encoder and decoder (aggregate them) and **prior** $p_\theta(z)$ is jointly inferred by decoder
  - Recall that the KL term is a function of $q_\phi(z|x)$ and $p_\theta(z)$

- **Inference:** Sample **prior** $p_\theta(z)$ from decoder and generate sample x

- NVAE [Vahdat et al., 2020]
  - **Idea 2.** Taming the unstable KL term

    1. Residual normal distribution
       - For each factorized **prior** distribution

         $$p(z_l^i|\boldsymbol{z}_{<l}) := \mathcal{N}(\mu_i(\boldsymbol{z}_{<l}), \sigma_i(\boldsymbol{z}_{<l})),$$

         define **approximate posterior** as (instead of directly predict μ_i, σ_i)

$$q(z_l^i|\boldsymbol{z}_{<l}, \boldsymbol{x}) := \mathcal{N}(\mu_i(\boldsymbol{z}_{<l}) + \Delta\mu_i(\boldsymbol{z}_{<l}, \boldsymbol{x}), \sigma_i(\boldsymbol{z}_{<l}) \cdot \Delta\sigma_i(\boldsymbol{z}_{<l}, \boldsymbol{x})),$$

       - Then, the **KL term** of ELBO is given by

$$\mathrm{KL}(q(z^i|\boldsymbol{x})||p(z^i)) = \frac{1}{2}\left(\frac{\Delta\mu_i^2}{\sigma_i^2} + \Delta\sigma_i^2 - \log\Delta\sigma_i^2 - 1\right)$$

    2. Spectral regularization
       - Enforce *Lipschitz smoothness* of encoder to bound KL divergence
       - Regularize the *largest singular value* of convolutional layers (estimated by power iteration [Yoshida & Miyato, 2017])

- NVAE [Vahdat et al., 2020]
  - **Results:**
    - Generate high-resolution (256x256) images

    - SOTA test negative log-likelihood (NLL) on non-autoregressive models

Method	**MNIST** 28×28	**CIFAR-10** 32×32	**ImageNet** 32×32	**CelebA** 64×64	**CelebA HQ** 256×256	**FFHQ** 256×256
NVAE w/o flow	**78.01**	2.93	-	2.04	-	0.71
NVAE w/ flow	78.19	**2.91**	3.92	**2.03**	**0.70**	**0.69**
VAE Models with an Unconditional Decoder						
BIVA [36]	78.41	3.08	3.96	2.48	-	-
IAF-VAE [4]	79.10	3.11	-	-	-	-
DVAE++ [20]	78.49	3.38	-	-	-	-
Conv Draw [42]	-	3.58	4.40	-	-	-
Flow Models without any Autoregressive Components in the Generative Model						
VFlow [59]	-	2.98	-	-	-	-
ANF [60]	-	3.05	3.92	-	0.72	-
Flow++ [61]	-	3.08	**3.86**	-	-	-
Residual flow [50]	-	3.28	4.01	-	0.99	-
GLOW [62]	-	3.35	4.09	-	1.03	-
Real NVP [63]	-	3.49	4.28	3.02	-	-

- Diffusion probabilistic models [Sohl-Dickstein et al., 2015]
  - Diffusion (forward) process: Markov chain that **gradually add noise** (of same dimension of data) to data until original the signal is destroyed

$$q(x_t|x_{t-1}) := \mathcal{N}(x_t; \sqrt{1-\beta_t}x_{t-1}, \beta_t I)$$

  - Sampling (backward) process: Markov chain with learned Gaussian **denoising transition**, starting from standard Gaussian noise $p(x_T) = \mathcal{N}(x_T; 0, I)$

$$p_\theta(x_{t-1}|x_t) := \mathcal{N}(x_{t-1}; \mu_\theta(x_t, t), \Sigma_\theta(x_t, t))$$

Denoising/sampling (reverse)

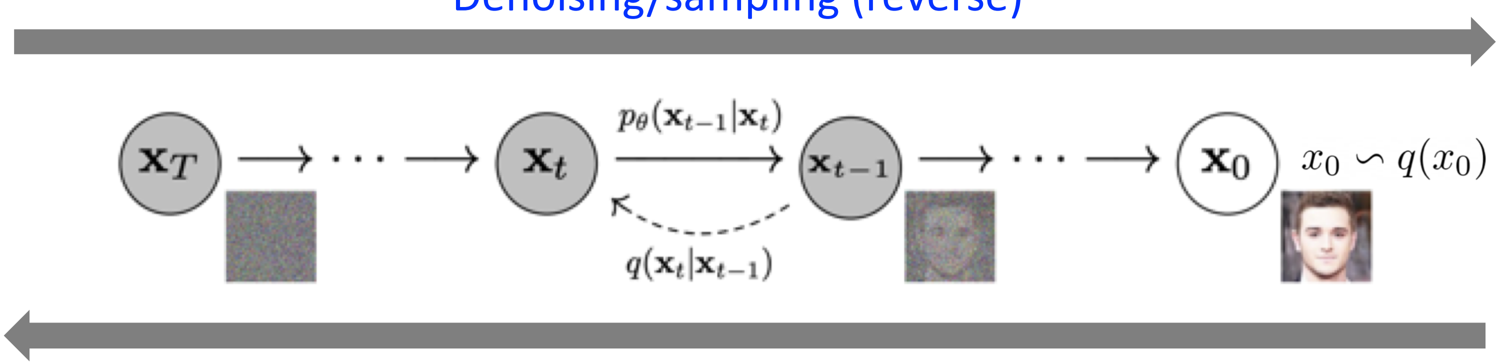

Diffusion process (forward)

- Diffusion probabilistic models [Sohl-Dickstein et al., 2015]
  - Here, the forward distribution $q(x_{t-1}|x_t, x_0)$ can be expressed as a closed form (composition of Gaussians)

  - **ELBO** objective is given by the sum of local KL divergences (between Gaussians)
    - Remark that both $q(x_{t-1}|x_t, x_0)$ and $p_\theta(x_{t-1}|x_t)$ are Gaussians

$$E_q[D_{\mathrm{KL}}(q(x_T|x_0)||p(x_T)) + \sum_{t>1} D_{\mathrm{KL}}(q(x_{t-1}|x_t, x_0)||p_\theta(x_{t-1}|x_t)) - \log p_\theta(x_0|x_1)]$$

  - DDPM [Ho et al., 2020] reparametrizes the model μ_θ as

$$\mu_\theta(x_t, t) := \alpha_t x_t + \gamma_t \epsilon_\theta(x_t, t)$$

    - Then, the training/sampling scheme resembles *denoising score matching* (will be discussed later in this lecture)
    - Intuitively, the reverse process adds the (learned) noise ϵ_θ for each step (resembles stochastic Langevin dynamics)

- Diffusion probabilistic models [Sohl-Dickstein et al., 2015]
  - DDPM achieved the SOTA FID score (3.17) on CIFAR-10 generation

  - DDPM also generates high-resolution (256x256) images

Table of Contents

- EBM [LeCun et al., 2006, Du & Mordatch, 2019]
  - Instead of directly modeling the density $p(x)$, learn the unnormalized density (i.e., energy) $E(x)$ such that

$$p_\theta(x) = \frac{\exp(-E_\theta(x))}{Z_\theta}, \quad Z_\theta = \int_{x \in \mathcal{X}} \exp(-E_\theta(x))$$

  - Here, we don't care about the **exact density** (which needs to compute the partition function Z_θ), but only interested in the **relative order** of densities

  - **Training:** The gradient of negative log-likelihood (NLL) is decomposed to:

$$\begin{aligned} \mathbb{E}_{x \sim p_{\mathtt{data}}(x)}[-\nabla_\theta \log p_\theta(x)] &= \mathbb{E}_{x \sim p_{\mathtt{data}}(x)}[\nabla_\theta E_\theta(x)] + \nabla_\theta \log Z_\theta \\ &= \underbrace{\mathbb{E}_{x \sim p_{\mathtt{data}}(x)}[\nabla_\theta E_\theta(x)]}_{\text{data gradient}} - \underbrace{\mathbb{E}_{x' \sim p_\theta(x)}[\nabla_\theta E_\theta(x')]}_{\text{model gradient}} \end{aligned}$$

  - Note that this **contrastive** objective resembles (Wasserstein) GAN, but EBM uses an implicit MCMC generating procedure and no gradient through sampling
    - One can modify the discriminator of GAN to be an EBM [Zhao et al., 2017]

- EBM [LeCun et al., 2006, Du & Mordatch, 2019]
  - Instead of directly modeling the density $p(x)$, learn the unnormalized density (i.e., energy) $E(x)$ such that

$$p_\theta(x) = \frac{\exp(-E_\theta(x))}{Z_\theta}, \quad Z_\theta = \int_{x \in \mathcal{X}} \exp(-E_\theta(x))$$

  - **Sampling:** Run Markov chain Monte Carlo (MCMC) to draw a sample from $p_\theta(x)$
    - For high-dimensional data (e.g., image generation), stochastic gradient Langevin dynamics (SGLD) [Welling & Teh, 2011] is popularly used:
      - Given an initial sample x^0, iteratively update x^{k+1} $(k = 0, \dots, K-1)$

$$x^{k+1} \leftarrow x^k + \frac{\alpha}{2} \underbrace{\nabla_x \log p_\theta(x^k)}_{-\nabla_x E_\theta(x)} + \epsilon, \quad \epsilon \sim \mathcal{N}(0, \alpha)$$

      - Due to the Gaussian noise, it does not collapse to the MAP solution but converges to $p_\theta(x)$ as $\alpha \to 0$ and $K \to \infty$

- **Advantages of EBMs**
  1. Compositionality: One can add or subtract multiple energy functions (e.g., male, black hair, smiling) to sample the composite distribution

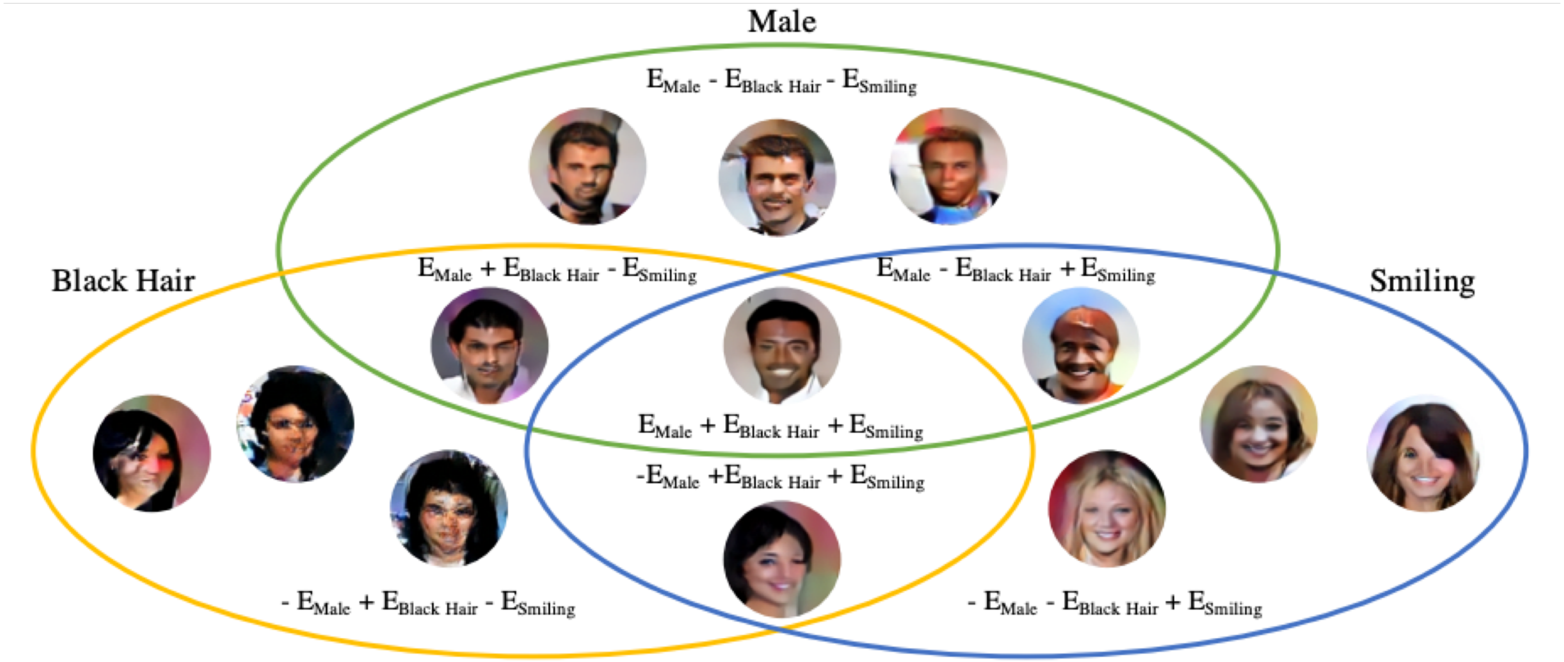

  2. No generator network: Unlike GAN/VAEs, EBMs do not need a specialized generator architecture (one can reuse the standard classifier architectures)
  3. Adaptive computation time: Since the sampling is given by iterative SGLD, the user can choose from the fast coarse samples to slow fine samples

- EBM [LeCun et al., 2006, Du & Mordatch, 2019]
  - The gradient of partition function can be reformulated as follow:

$$
\begin{aligned}
\nabla_{\boldsymbol{\theta}} \log Z_{\boldsymbol{\theta}} &= \nabla_{\boldsymbol{\theta}} \log \int \exp(-E_{\boldsymbol{\theta}}(\mathbf{x}))d\mathbf{x} \\
&\overset{(i)}{=} \left(\int \exp(-E_{\boldsymbol{\theta}}(\mathbf{x}))d\mathbf{x}\right)^{-1} \nabla_{\boldsymbol{\theta}} \int \exp(-E_{\boldsymbol{\theta}}(\mathbf{x}))d\mathbf{x} \\
&= \left(\int \exp(-E_{\boldsymbol{\theta}}(\mathbf{x}))d\mathbf{x}\right)^{-1} \int \nabla_{\boldsymbol{\theta}} \exp(-E_{\boldsymbol{\theta}}(\mathbf{x}))d\mathbf{x} \\
&\overset{(ii)}{=} \left(\int \exp(-E_{\boldsymbol{\theta}}(\mathbf{x}))d\mathbf{x}\right)^{-1} \int \exp(-E_{\boldsymbol{\theta}}(\mathbf{x}))(-\nabla_{\boldsymbol{\theta}} E_{\boldsymbol{\theta}}(\mathbf{x}))d\mathbf{x} \\
&= \int \left(\int \exp(-E_{\boldsymbol{\theta}}(\mathbf{x}))d\mathbf{x}\right)^{-1} \exp(-E_{\boldsymbol{\theta}}(\mathbf{x}))(-\nabla_{\boldsymbol{\theta}} E_{\boldsymbol{\theta}}(\mathbf{x}))d\mathbf{x} \\
&\overset{(iii)}{=} \int \frac{\exp(-E_{\boldsymbol{\theta}}(\mathbf{x}))}{Z_{\boldsymbol{\theta}}}(-\nabla_{\boldsymbol{\theta}} E_{\boldsymbol{\theta}}(\mathbf{x}))d\mathbf{x} \\
&\overset{(iv)}{=} \int p_{\boldsymbol{\theta}}(\mathbf{x})(-\nabla_{\boldsymbol{\theta}} E_{\boldsymbol{\theta}}(\mathbf{x}))d\mathbf{x} \\
&= \mathbb{E}_{\mathbf{x} \sim p_{\boldsymbol{\theta}}(\mathbf{x})} \left[-\nabla_{\boldsymbol{\theta}} E_{\boldsymbol{\theta}}(\mathbf{x})\right],
\end{aligned}
$$

Joint Energy-based Models (JEM)

- JEM [Grathwohl et al., 2020]
  - Use standard classifier architectures for *joint distribution* EBMs
  - Recall that the classifier $p_\theta(y|x)$ is expressed by the logits $f_\theta(x)$

$$p_\theta(y|x) = \frac{\exp(f_\theta(x)[y])}{\sum_{y'} \exp(f_\theta(x)[y'])}$$

  - Here, one can re-interpret the logits to define an energy-based model

$$p_\theta(x,y) = \frac{\exp(f_\theta(x)[y])}{Z_\theta}, \quad p_\theta(x) = \frac{\sum_y \exp(f_\theta(x)[y])}{Z_\theta}$$

  - Note that shifting the logits does not affect $p_\theta(y|x)$ but $p_\theta(x)$; hence, EBM gives an extra degree of freedom
  - The objective of JEM is a **sum** of density and conditional models, where the density model is trained by contrastive objective of EBM

$$\log p_\theta(x,y) = \log p_\theta(x) + \log p_\theta(y|x)$$

- JEM [Grathwohl et al., 2020]
  - JEM achieves a competitive performance as both classifier and generative model

Class	Model	Accuracy% ↑	IS↑	FID↓
Hybrid	Residual Flow	70.3	3.6	46.4
	Glow	67.6	3.92	48.9
	IGEBM	49.1	8.3	**37.9**
	JEM $p(\mathbf{x}\|y)$ factored	30.1	6.36	61.8
	JEM (Ours)	**92.9**	**8.76**	38.4
Disc.	Wide-Resnet	95.8	N/A	N/A
Gen.	SNGAN	N/A	8.59	25.5
	NCSN	N/A	8.91	25.32

  - Also, JEM (generative classifier) improves uncertainty and robustness
    - (a) calibration, (b) out-of-distribution detection, (c) adversarial robustness

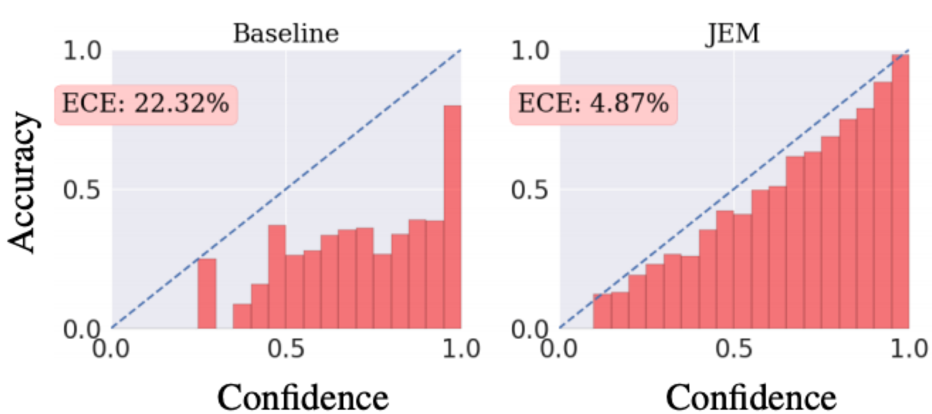

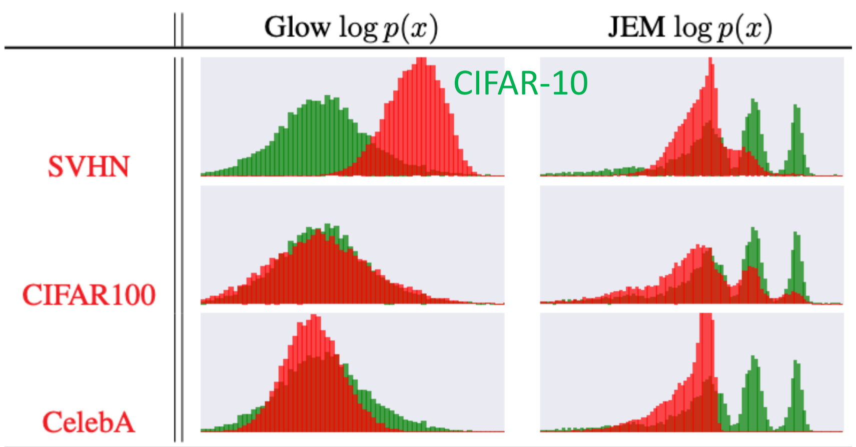

Score Matching

- Score matching [Hyvärinen, 2005]
  - Score = gradient of the log-likelihood $s(x) \coloneqq \nabla_x \log p(x)$
  - Score matching = Match the *scores* of data and model distribution
    - However, we **don't know** the scores of data distribution
    - Instead, one can use the **equivalent form** (proof by integration of parts)

$$\frac{1}{2}\mathbb{E}_{x\sim p_{\texttt{data}}(x)}[\|s_\theta(x) - s_{\texttt{data}}(x)\|_2^2] = \mathbb{E}_{x\sim p_{\texttt{data}}(x)}\left[\mathrm{tr}(\nabla_x s_\theta(x)) + \frac{1}{2}\|s_\theta(x)\|_2^2\right] + \text{const.}$$

🤔 😀

  - Recent works mostly consider **denoising score matching** [Vincent, 2011]
    - Match the score of **perturbed distribution** $q_\sigma(\tilde{x}) \coloneqq \int q_\sigma(\tilde{x}|x)\, p_{\text{data}}(x)$ where $q_\sigma(\tilde{x}|x) = \mathcal{N}(x, \sigma)$
    - Then, the score matching objective is **equivalent** to

$$\frac{1}{2}\mathbb{E}_{\tilde{x}\sim q_\sigma(\tilde{x}|x)p_{\texttt{data}}(x)}[\|s_\theta(\tilde{x}) - \nabla_{\tilde{x}} \log q_\sigma(\tilde{x}|x)\|_2^2]$$

    - It is tractable since the gradient $\nabla_{\tilde{x}} \log q_\sigma(\tilde{x}|x) = \nabla_{\tilde{x}} \log \mathcal{N}(\tilde{x}|x,\sigma) = \nabla_{\tilde{x}} \log \frac{1}{\sigma\sqrt{2\pi}} \exp(-\frac{1}{2}(\frac{\tilde{x}-x}{\sigma})^2)$ can be **analytically computed**
    - The objective can learn the scores of data distribution if $\sigma \approx 0$

- Score matching [Hyvärinen, 2005]
  - The score matching objective can be reformulated as follow:

$$\frac{1}{2}\mathbb{E}_{x\sim p_{\texttt{data}}(x)}[\|s_\theta(x) - s_{\texttt{data}}(x)\|_2^2] = \mathbb{E}_{x\sim p_{\texttt{data}}(x)}\left[\mathrm{tr}(\nabla_x s_\theta(x)) + \frac{1}{2}\|s_\theta(x)\|_2^2\right] + \mathrm{const.}$$

  - It is sufficient to show that

$$\begin{aligned}\mathbb{E}_{p_{\texttt{data}}(x)}[-s_{\texttt{data}}(x)s_\theta(x)] &= \sum_i \int -p_{\texttt{data}}(x)\frac{\partial \log p_{\texttt{data}}(x)}{dx_i}s_{\theta,i}(x)dx \\ &= \sum_i \int -\frac{\partial p_{\texttt{data}}(x)}{dx_i}s_{\theta,i}(x)dx \\ &= \sum_i \int p_{\texttt{data}}(x)\frac{\partial s_{\theta,i}(x)}{dx_i}dx + \mathrm{const.}\end{aligned}$$

  - The last equality comes from the integration of parts

$$\int p'(x)f(x)dx = p(x)f(x)\Big|_{-\infty}^{\infty} - \int p(x)f'(x)dx$$

and assumption $p_{\text{data}}(x)s_\theta(x) \to 0$ for both side of infinity

- NCSN [Song et al., 2019]
  - Previous works mostly define the score as a gradient of the **energy function** $s_\theta(x) \coloneqq -\nabla_x E_\theta(x)$
  - This work: **Directly model** the score $x \in \mathbb{R}^d \mapsto s_\theta(x) \in \mathbb{R}^d$ as an output

- **Noise-conditional Score Network**
  - Denoising score matching is stable for large σ but unbiased for small σ
  - **Idea:** Learn multiple noise levels (with a single neural network) and anneal the noise level during sampling $\sigma_1 > \cdots > \sigma_L$

Algorithm 1 Annealed Langevin dynamics.

Require: $\{\sigma_i\}_{i=1}^L, \epsilon, T$.

Initialize $\tilde{\mathbf{x}}_0$
for $i \leftarrow 1$ to L **do**
  $\alpha_i \leftarrow \epsilon \cdot \sigma_i^2/\sigma_L^2$ ▷ α_i is the step size.
  for $t \leftarrow 1$ to T **do**
    Draw $\mathbf{z}_t \sim \mathcal{N}(0, I)$
    $\tilde{\mathbf{x}}_t \leftarrow \tilde{\mathbf{x}}_{t-1} + \frac{\alpha_i}{2}\mathbf{s}_{\boldsymbol{\theta}}(\tilde{\mathbf{x}}_{t-1}, \sigma_i) + \sqrt{\alpha_i}\,\mathbf{z}_t$
  end for
  $\tilde{\mathbf{x}}_0 \leftarrow \tilde{\mathbf{x}}_T$
end for
return $\tilde{\mathbf{x}}_T$

- One can extend score matching to **continuous version** (stochastic differential equations, SDEs) [Song et al., 2021]
  - NCSN and DDPM can be viewed as different discretization of some SDEs
  - This view provides a better approach for **generation** and **likelihood estimation**

See Appendix for details

Noise-conditional Score Network (NCSN)

- NCSN [Song et al., 2019]
  - The continuous version of NCSN [Song et al., 2021] is SOTA for both **likelihood estimation** and **sample generation** on CIFAR-10

Table 2: NLLs and FIDs (ODE) on CIFAR-10.

Model	NLL Test ↓	FID ↓
RealNVP (Dinh et al., 2016)	3.49	-
iResNet (Behrmann et al., 2019)	3.45	-
Glow (Kingma & Dhariwal, 2018)	3.35	-
MintNet (Song et al., 2019b)	3.32	-
Residual Flow (Chen et al., 2019)	3.28	46.37
FFJORD (Grathwohl et al., 2018)	3.40	-
Flow++ (Ho et al., 2019)	3.29	-
DDPM (L) (Ho et al., 2020)	$\leqslant 3.70^*$	13.51
DDPM (L_{simple}) (Ho et al., 2020)	$\leqslant 3.75^*$	3.17
DDPM	3.28	3.37
DDPM cont. (VP)	3.21	3.69
DDPM cont. (sub-VP)	3.05	3.56
DDPM++ cont. (VP)	3.16	3.93
DDPM++ cont. (sub-VP)	3.02	3.16
DDPM++ cont. (deep, VP)	3.13	3.08
DDPM++ cont. (deep, sub-VP)	**2.99**	**2.92**

Table 3: CIFAR-10 sample quality.

Model	FID↓	IS↑
Conditional		
BigGAN (Brock et al., 2018)	14.73	9.22
StyleGAN2-ADA (Karras et al., 2020a)	**2.42**	**10.14**
Unconditional		
StyleGAN2-ADA (Karras et al., 2020a)	2.92	9.83
NCSN (Song & Ermon, 2019)	25.32	$8.87 \pm .12$
NCSNv2 (Song & Ermon, 2020)	10.87	$8.40 \pm .07$
DDPM (Ho et al., 2020)	3.17	$9.46 \pm .11$
DDPM++	2.78	9.64
DDPM++ cont. (VP)	2.55	9.58
DDPM++ cont. (sub-VP)	2.61	9.56
DDPM++ cont. (deep, VP)	2.41	9.68
DDPM++ cont. (deep, sub-VP)	2.41	9.57
NCSN++	2.45	9.73
NCSN++ cont. (VE)	2.38	9.83
NCSN++ cont. (deep, VE)	**2.20**	**9.89**

- Score matching through SDE [Song et al., 2021]

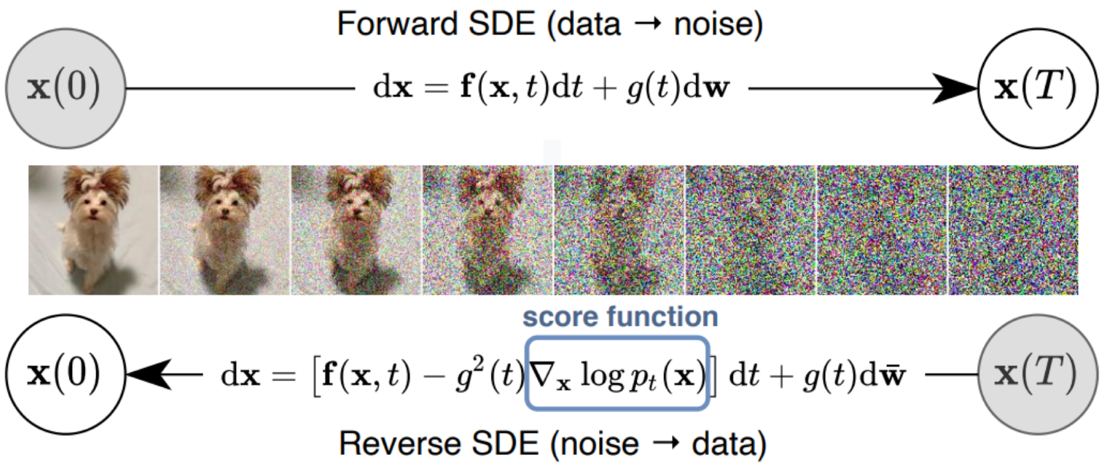

- Like DDPM, we consider some forward diffusion process (SDE):

$$\mathrm{d}\mathbf{x} = [\mathbf{f}(\mathbf{x}, t) - g(t)^2 \nabla_{\mathbf{x}} \log p_t(\mathbf{x})]\mathrm{d}t + g(t)\mathrm{d}\bar{\mathbf{w}},$$

- Then, the reverse diffusion process also follows some SDE:

$$\mathrm{d}\mathbf{x} = [\mathbf{f}(\mathbf{x}, t) - g(t)^2 \nabla_{\mathbf{x}} \log p_t(\mathbf{x})]\mathrm{d}t + g(t)\mathrm{d}\bar{\mathbf{w}},$$

- One can learn the score function by score matching

$$\boldsymbol{\theta}^* = \arg\min_{\boldsymbol{\theta}} \mathbb{E}_t \Big\{ \lambda(t) \mathbb{E}_{\mathbf{x}(0)} \mathbb{E}_{\mathbf{x}(t)|\mathbf{x}(0)} \Big[\big\| \mathbf{s}_{\boldsymbol{\theta}}(\mathbf{x}(t), t) - \nabla_{\mathbf{x}(t)} \log p_{0t}(\mathbf{x}(t) \mid \mathbf{x}(0)) \big\|_2^2 \Big] \Big\}.$$

- Score matching through SDE [Song et al., 2021]

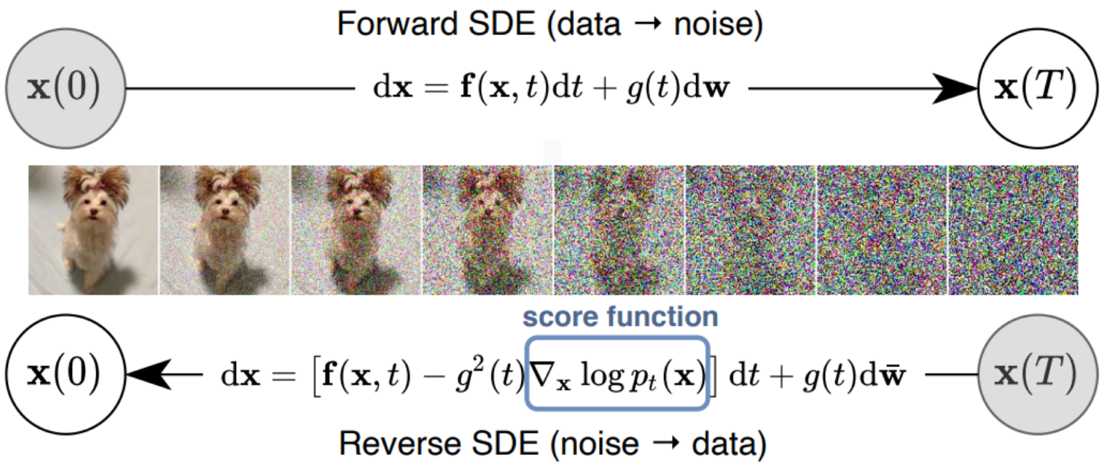

  - Like DDPM, we consider some forward diffusion process (SDE):

$$\mathrm{d}\mathbf{x} = [\mathbf{f}(\mathbf{x}, t) - g(t)^2 \nabla_{\mathbf{x}} \log p_t(\mathbf{x})]\mathrm{d}t + g(t)\mathrm{d}\bar{\mathbf{w}},$$

  - Here, NCSN and DDPM can be viewed as different discretizations some stochastic differential equations (SDEs)

    - NCSN: $\mathrm{d}\mathbf{x} = \sqrt{\frac{\mathrm{d}\left[\sigma^2(t)\right]}{\mathrm{d}t}}\mathrm{d}\mathbf{w}$ $\rightarrow$ $\mathbf{x}_i = \mathbf{x}_{i-1} + \sqrt{\sigma_i^2 - \sigma_{i-1}^2}\mathbf{z}_i$
    - DDPM: $\mathrm{d}\mathbf{x} = -\frac{1}{2}\beta(t)\mathbf{x}\,\mathrm{d}t + \sqrt{\beta(t)}\,\mathrm{d}\mathbf{w}$ $\rightarrow$ $\mathbf{x}_i = \sqrt{1-\beta_i}\mathbf{x}_{i-1} + \sqrt{\beta_i}\mathbf{z}_i$

- Score matching through SDE [Song et al., 2021]
  - The reverse diffusion process can be solved by **3 ways**:

1. Run a general-purpose SDE solver (a.k.a. predictor)
2. Utilize the score-based model $s_\theta(x,t) \approx \nabla_x \log p_t(x)$ (a.k.a. corrector)

→ Combining predictor and corrector gives the **SOTA generation** performance

Algorithm 2 PC sampling (VE SDE)

1: $\mathbf{x}_N \sim \mathcal{N}(\mathbf{0}, \sigma_{\max}^2 \mathbf{I})$
2: **for** $i = N-1$ **to** 0 **do**
3: $\quad \mathbf{x}_i' \leftarrow \mathbf{x}_{i+1} + (\sigma_{i+1}^2 - \sigma_i^2)\mathbf{s}_{\boldsymbol{\theta}^*}(\mathbf{x}_{i+1}, \sigma_{i+1})$
4: $\quad \mathbf{z} \sim \mathcal{N}(\mathbf{0}, \mathbf{I})$
5: $\quad \mathbf{x}_i \leftarrow \mathbf{x}_i' + \sqrt{\sigma_{i+1}^2 - \sigma_i^2}\,\mathbf{z}$
6: $\quad$ **for** $j = 1$ **to** M **do**
7: $\quad\quad \mathbf{z} \sim \mathcal{N}(\mathbf{0}, \mathbf{I})$
8: $\quad\quad \mathbf{x}_i \leftarrow \mathbf{x}_i + \epsilon_i \mathbf{s}_{\boldsymbol{\theta}^*}(\mathbf{x}_i, \sigma_i) + \sqrt{2\epsilon_i}\,\mathbf{z}$
9: **return** $\mathbf{x}_0$

Continuous ver. of NCSN

Algorithm 3 PC sampling (VP SDE)

1: $\mathbf{x}_N \sim \mathcal{N}(\mathbf{0}, \mathbf{I})$
2: **for** $i = N-1$ **to** 0 **do**
3: $\quad \mathbf{x}_i' \leftarrow (2 - \sqrt{1-\beta_{i+1}})\mathbf{x}_{i+1} + \beta_{i+1}\mathbf{s}_{\boldsymbol{\theta}^*}(\mathbf{x}_{i+1}, i+1)$
4: $\quad \mathbf{z} \sim \mathcal{N}(\mathbf{0}, \mathbf{I})$
5: $\quad \mathbf{x}_i \leftarrow \mathbf{x}_i' + \sqrt{\beta_{i+1}}\,\mathbf{z}$
6: $\quad$ **for** $j = 1$ **to** M **do**
7: $\quad\quad \mathbf{z} \sim \mathcal{N}(\mathbf{0}, \mathbf{I})$
8: $\quad\quad \mathbf{x}_i \leftarrow \mathbf{x}_i + \epsilon_i \mathbf{s}_{\boldsymbol{\theta}^*}(\mathbf{x}_i, i) + \sqrt{2\epsilon_i}\,\mathbf{z}$
9: **return** $\mathbf{x}_0$

Predictor

Corrector

Continuous ver. of DDPM

- Score matching through SDE [Song et al., 2021]
  - The reverse diffusion process can be solved by **3 ways**:

1. Run a general-purpose SDE solver (a.k.a. predictor)
2. Utilize the score-based model $s_\theta(x,t) \approx \nabla_x \log p_t(x)$ (a.k.a. corrector)

3. Convert to deterministic ODE
   - Every SDE (Ito process) has a corresponding deterministic ODE

$$\mathrm{d}\mathbf{x} = \left[\mathbf{f}(\mathbf{x},t) - \frac{1}{2}g(t)^2\nabla_{\mathbf{x}}\log p_t(\mathbf{x})\right]\mathrm{d}t,$$

     whose trajectories include the same evolution of densities

   - Deterministic ODE defines an invertible model (a.k.a. normalizing flow) [Chen et al., 2018]
   - Using this formulation, one can
     a) Compute exact likelihood
     b) Manipulate latents with encoder (model is invertible)

Autoregressive models

- Autoregressive generation (e.g., pixel-by-pixel for images) :

$$p(\boldsymbol{x}) = \prod_{k=1}^{K^2} p(x_k | x_1, \cdots, x_{k-1})$$
$$= \prod_{k=1}^{K^2} p(x_k | \boldsymbol{x}_{<k})$$

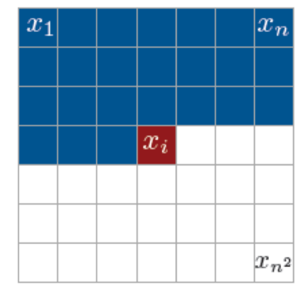

- For example, each RBG pixel is generated autoregressively:

$$p(x_k | \boldsymbol{x}_{<k}) = p(x_{k,R}, x_{k,B}, x_{k,G} | \boldsymbol{x}_{<k})$$
$$= p(x_{k,R} | \boldsymbol{x}_{<k}) p(x_{k,B} | \boldsymbol{x}_{<k}, x_{k,R}) p(x_{k,G} | \boldsymbol{x}_{<k}, x_{k,R}, x_{k,B})$$

- Each pixel is treated as discrete variables, sampled from softmax distributions:

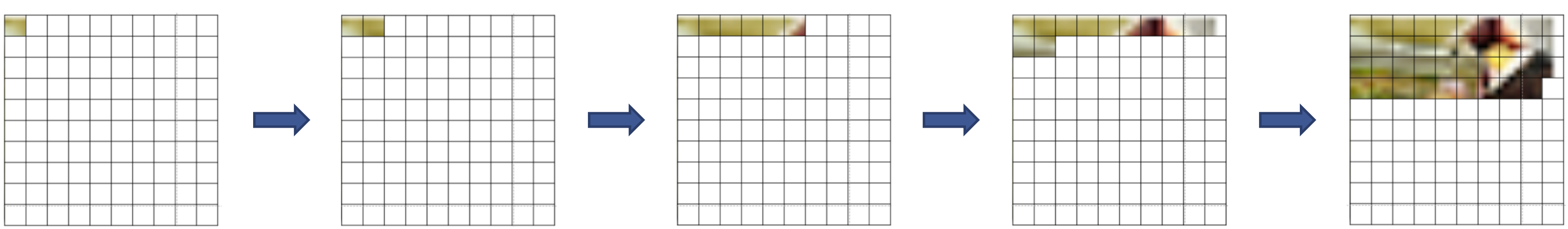

Pixel Convolutional/Recurrent Neural Network (PixelCNN/PixelRNN)

- Using CNN and RNN for modeling $p(x_k|\boldsymbol{x}_{<k})$ [Oord et al., 2016]
  - Simply treating $\boldsymbol{x}_{<k}$ as one-dimensional (instead of two-dimensional) vector:

CNN-based

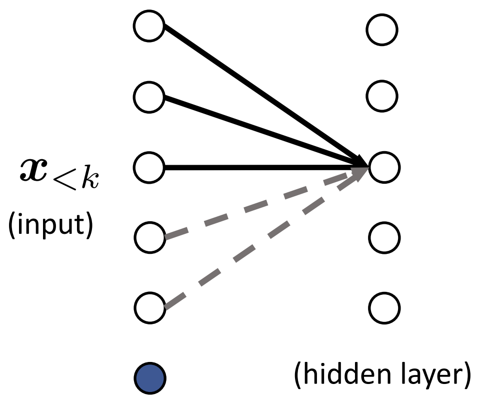

masked convolution

- Using CNN and RNN for modeling $p(x_k|\boldsymbol{x}_{<k})$ [Oord et al., 2016]
  - Simply treating $\boldsymbol{x}_{<k}$ as one-dimensional (instead of two-dimensional) vector:

CNN-based

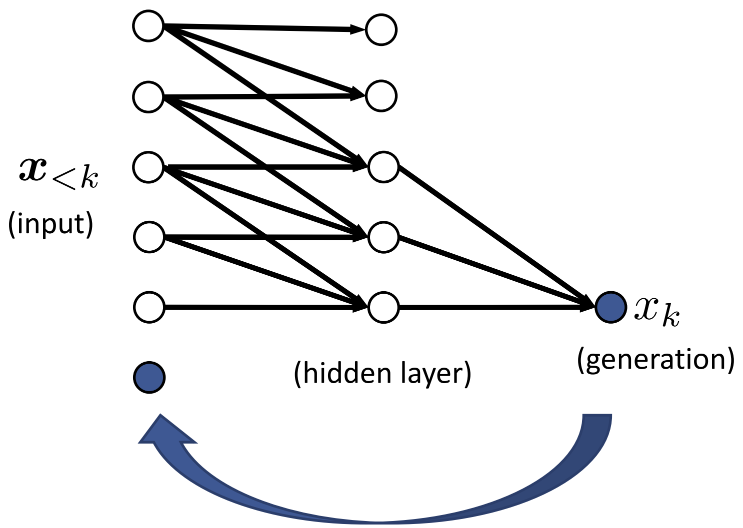

Pixel Convolutional/Recurrent Neural Network (PixelCNN/PixelRNN)

- Using CNN and RNN for modeling $p(x_k|\boldsymbol{x}_{<k})$ [Oord et al., 2016]
  - Simply treating $\boldsymbol{x}_{<k}$ as one-dimensional (instead of two-dimensional) vector:

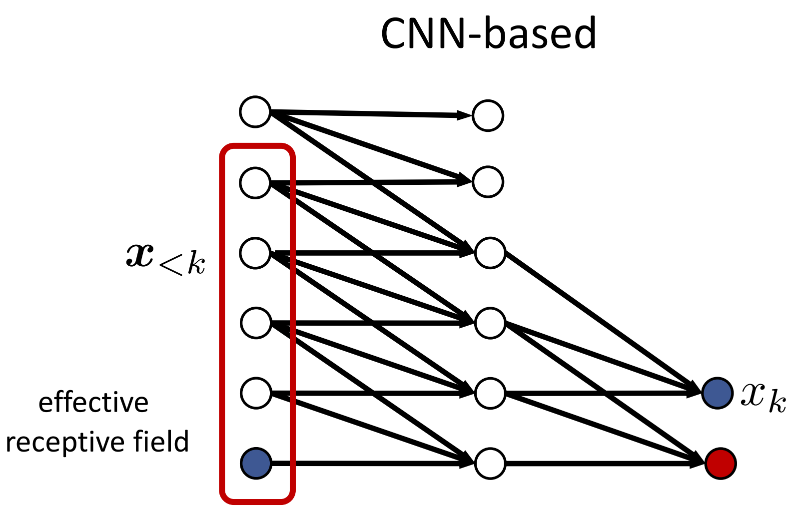

- Using CNN and RNN for modeling $p(x_k|\boldsymbol{x}_{<k})$ [Oord et al., 2016]
  - Simply treating $\boldsymbol{x}_{<k}$ as one-dimensional (instead of two-dimensional) vector:

CNN-based

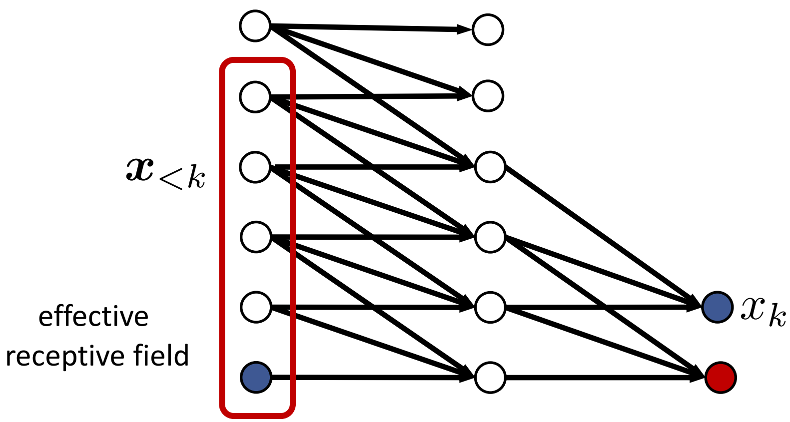

RNN-based

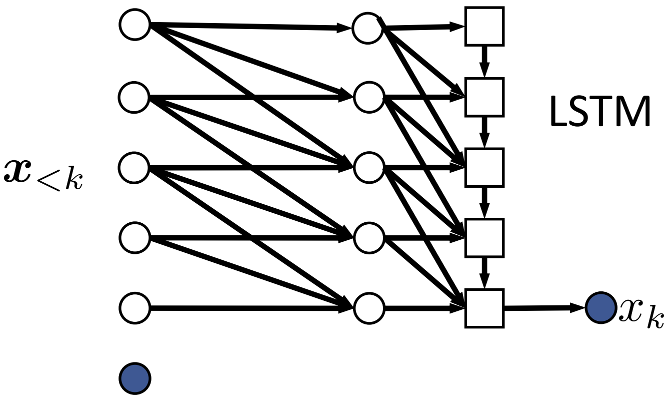

- Using CNN and RNN for modeling $p(x_k|\boldsymbol{x}_{<k})$ [Oord et al., 2016]
  - Simply treating $\boldsymbol{x}_{<k}$ as one-dimensional (instead of two-dimensional) vector:

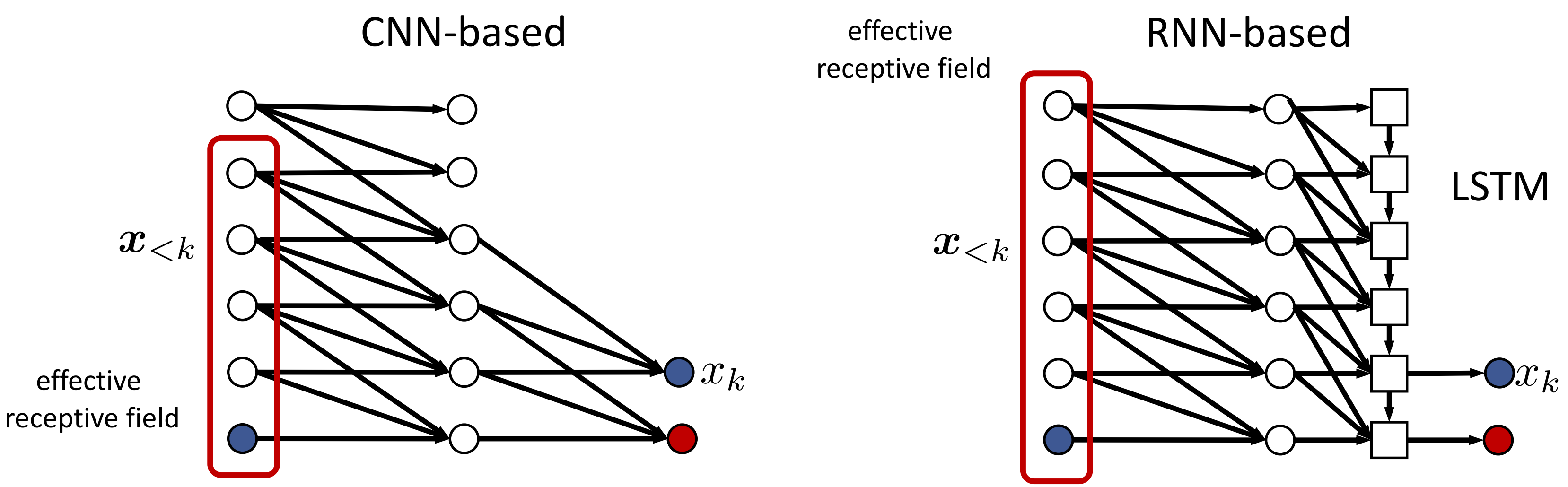

- **Inference** requires iterative forward procedure (slow)
- **Training** requires single forward pass for CNN, but multiple pass for RNN (slow)
- Effective receptive field (context of pixel generation) is unbounded for RNN, but bounded for CNN (constrained)

Next, extending to two-dimensional data

- Using CNN and RNN for modeling $p(x_k|\boldsymbol{x}_{<k})$ [Oord et al., 2016]
    - Pixel CNN use masked convolutional layer (for $\boldsymbol{x}_{>k}$)

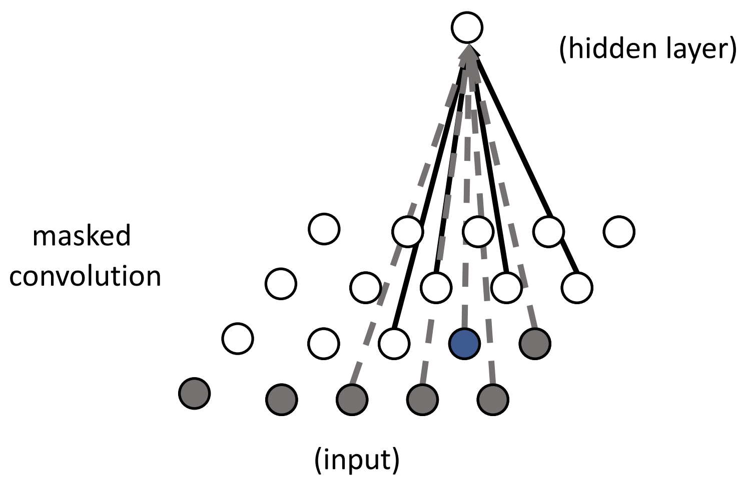

Pixel CNN

- Using CNN and RNN for modeling $p(x_k|\boldsymbol{x}_{<k})$ [Oord et al., 2016]
  - Pixel CNN use masked convolutional layer (for $\boldsymbol{x}_{>k}$)

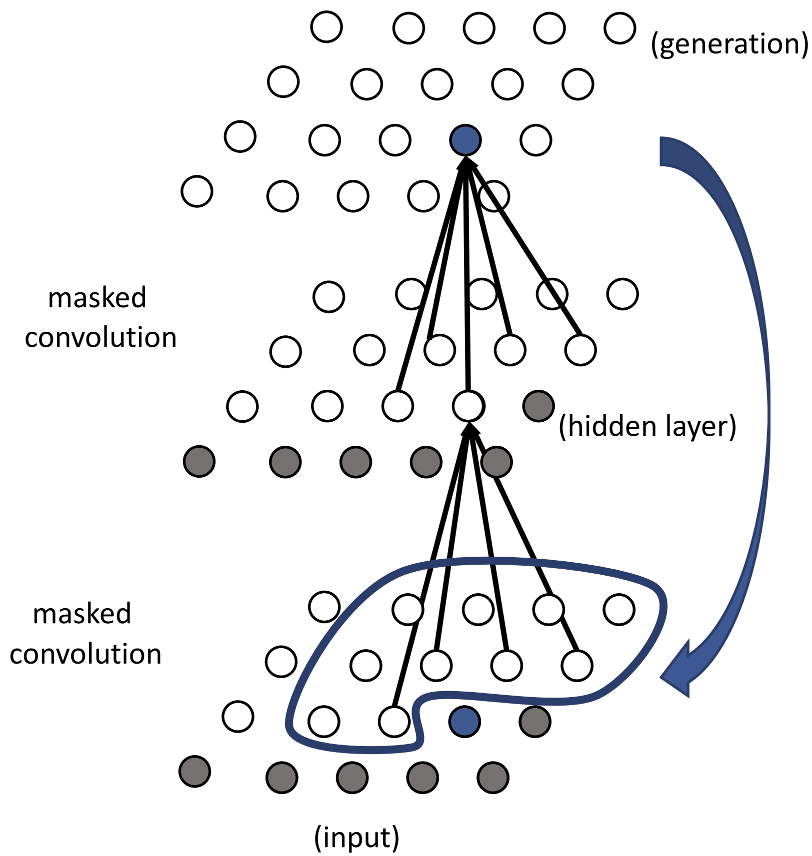

Pixel CNN

- Using CNN and RNN for modeling $p(x_k|\boldsymbol{x}_{<k})$ [Oord et al., 2016]
  - Pixel CNN use masked convolutional layer (for $\boldsymbol{x}_{>k}$)
  - Row LSTM use LSTMs, generating image row-by-row (not pixel-by-pixel)

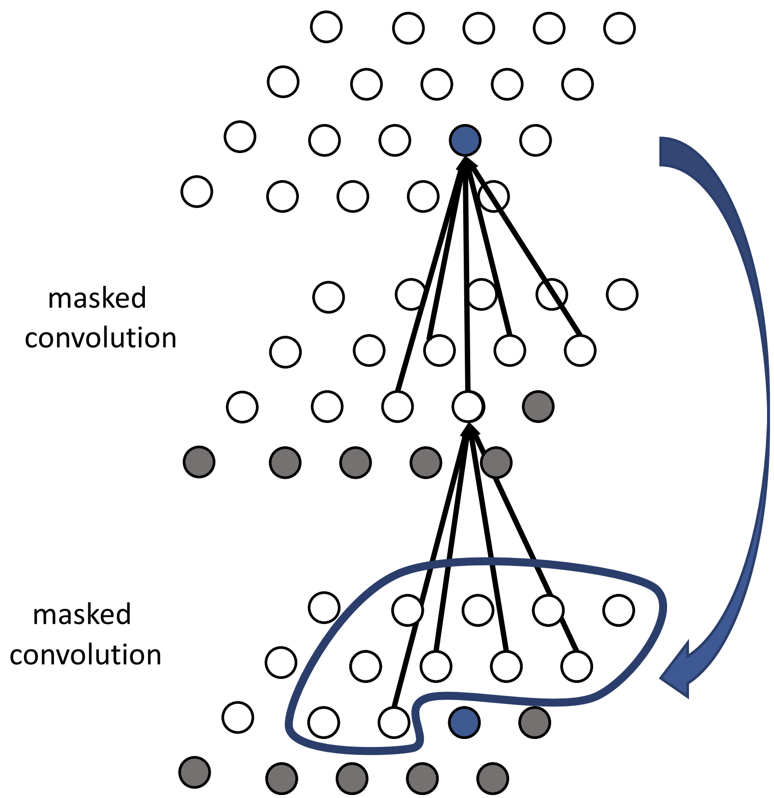

Pixel CNN

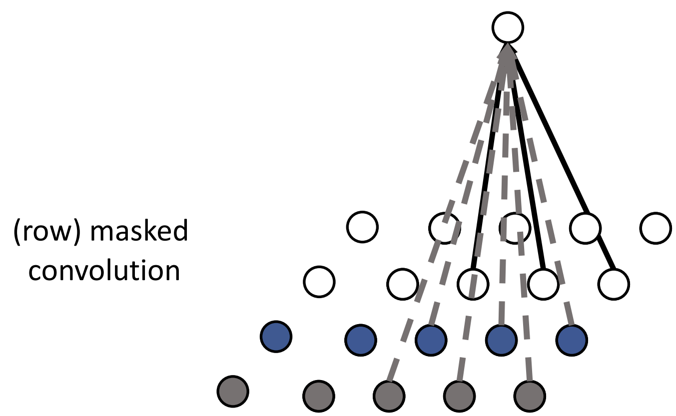

Row LSTM

- Using CNN and RNN for modeling $p(x_k|\boldsymbol{x}_{<k})$ [Oord et al., 2016]
  - Pixel CNN use masked convolutional layer (for $\boldsymbol{x}_{>k}$)
  - Row LSTM use LSTMs, generating image row-by-row (not pixel-by-pixel)

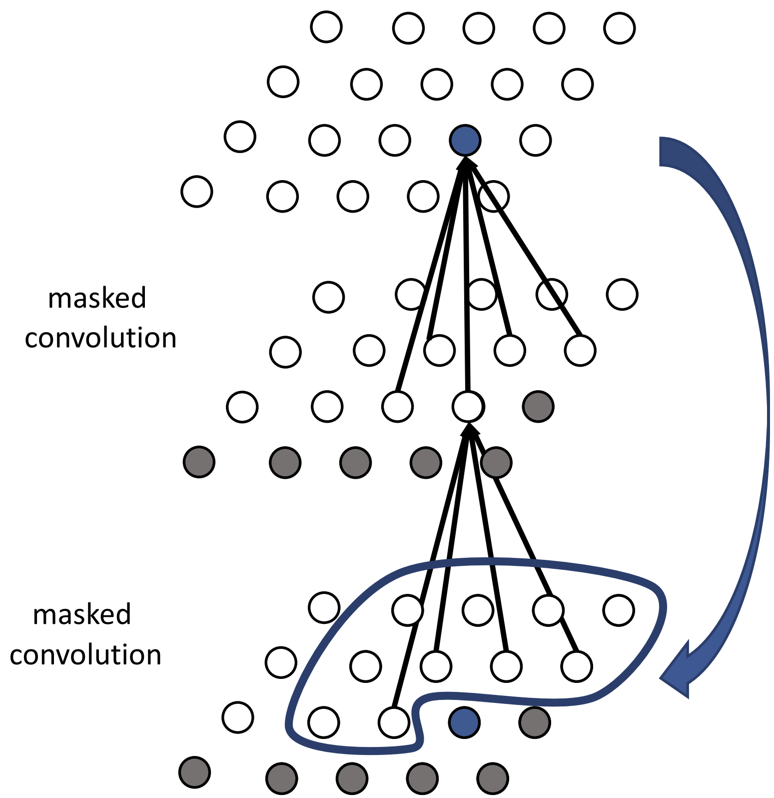

Pixel CNN

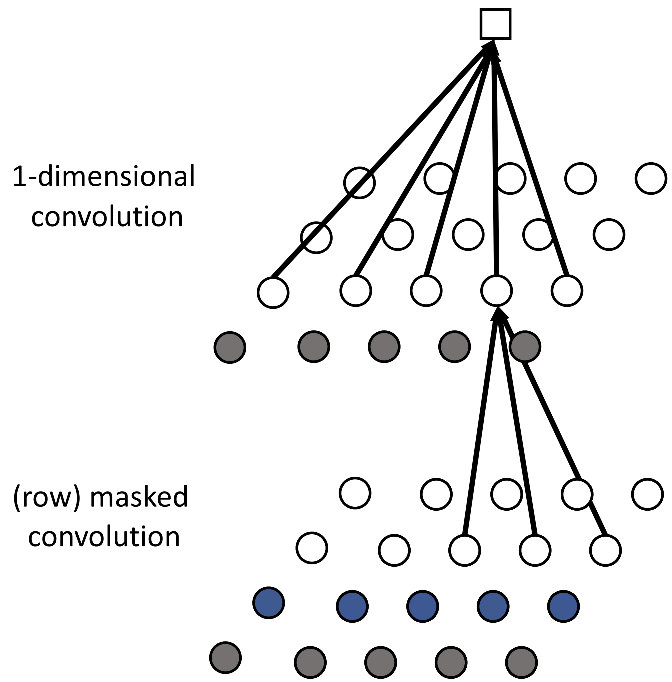

Row LSTM

- Using CNN and RNN for modeling $p(x_k|\boldsymbol{x}_{<k})$ [Oord et al., 2016]
  - Pixel CNN use masked convolutional layer (for $\boldsymbol{x}_{>k}$)
  - Row LSTM use LSTMs, generating image row-by-row (not pixel-by-pixel)

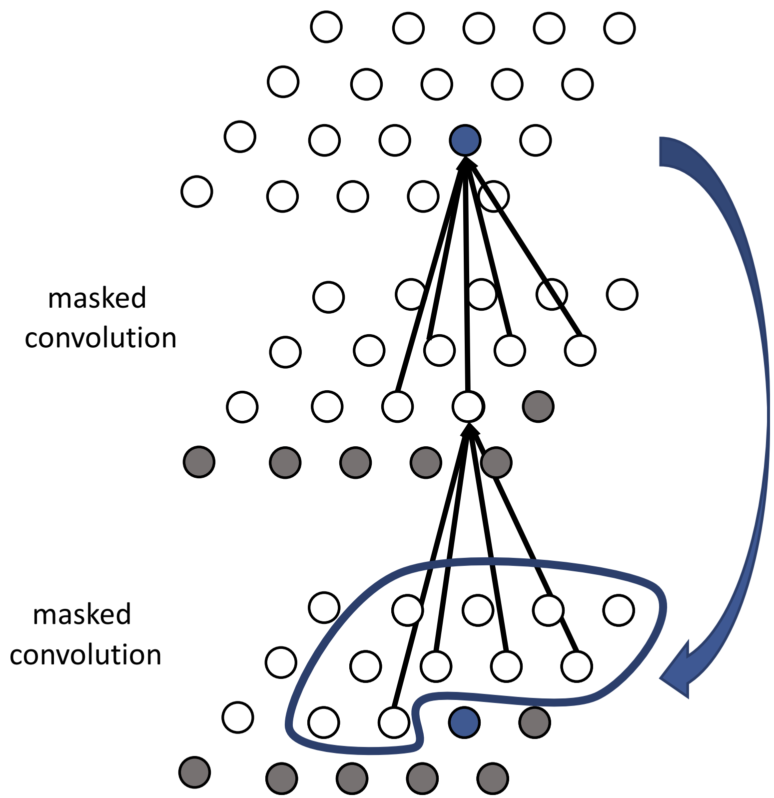

Pixel CNN

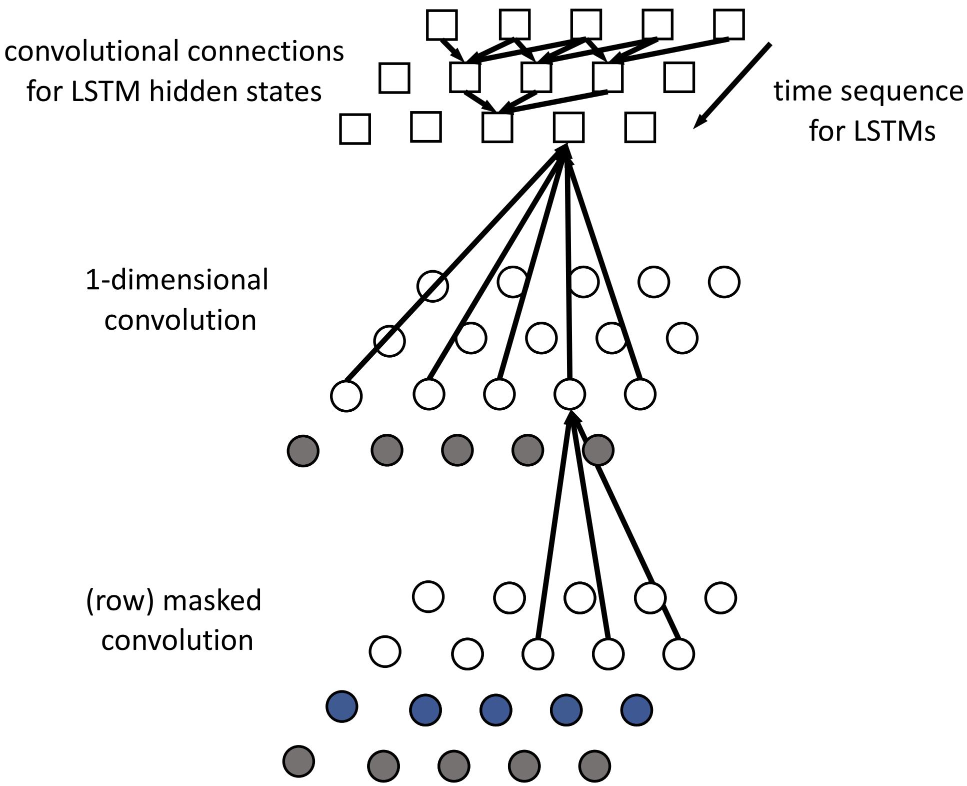

Row LSTM

Pixel Convolutional/Recurrent Neural Network (PixelCNN/PixelRNN)

- Using CNN and RNN for modeling $p(x_k|\boldsymbol{x}_{<k})$ [Oord et al., 2016]
  - Pixel CNN use masked convolutional layer (for $\boldsymbol{x}_{>k}$)
  - Row LSTM use LSTMs, generating image row-by-row (not pixel-by-pixel)

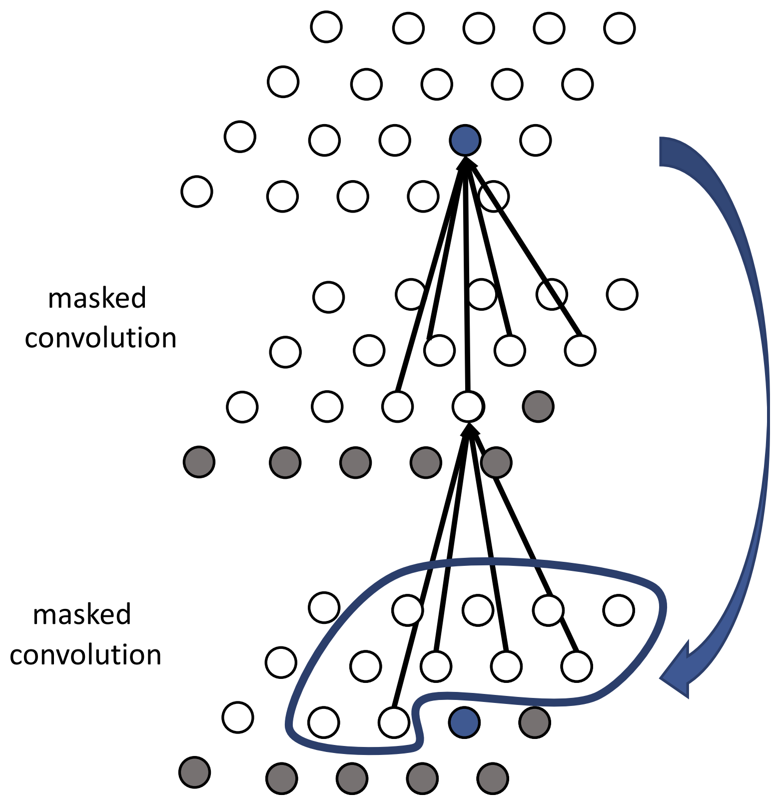

Pixel CNN

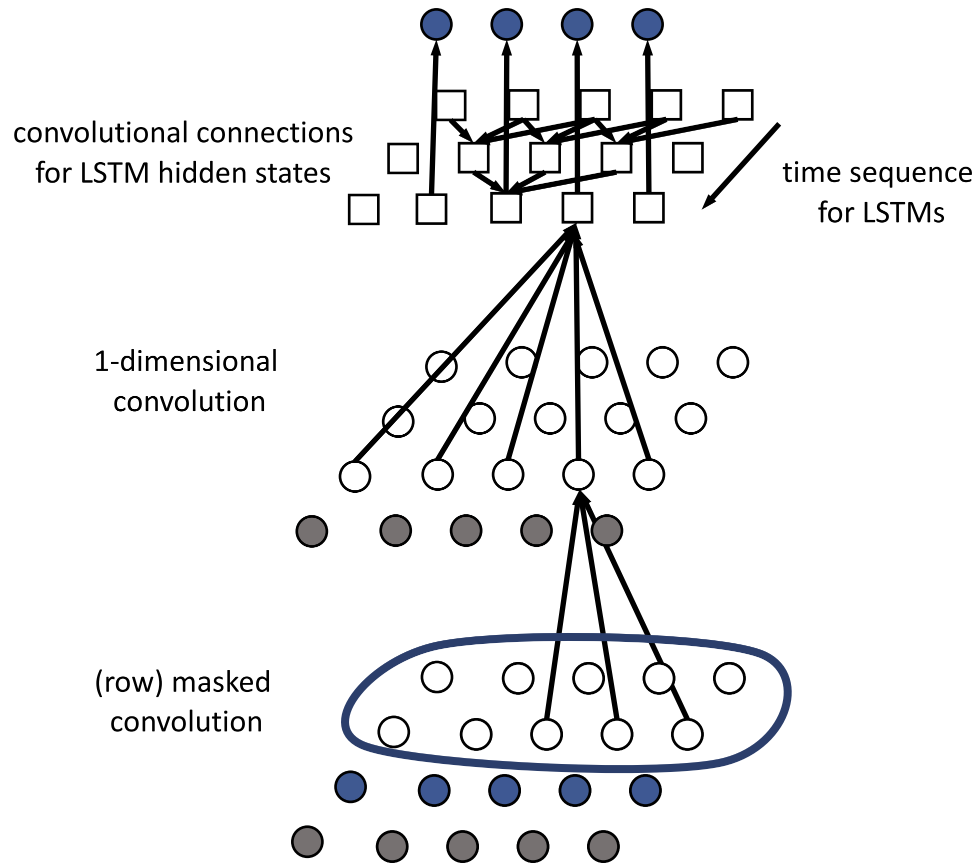

Row LSTM

Next, introducing column-wise dependencies using LSTMs

- Using CNN and RNN for modeling $p(x_k|\boldsymbol{x}_{<k})$ [Oord et al., 2016]
  - Pixel CNN use masked convolutional layer (for $\boldsymbol{x}_{>k}$)
  - Row LSTM use LSTMs, generating image row-by-row (not pixel-by-pixel)
  - Diagonal BiLSTM use bi-directional LSTMs, to generate image pixel-by-pixel

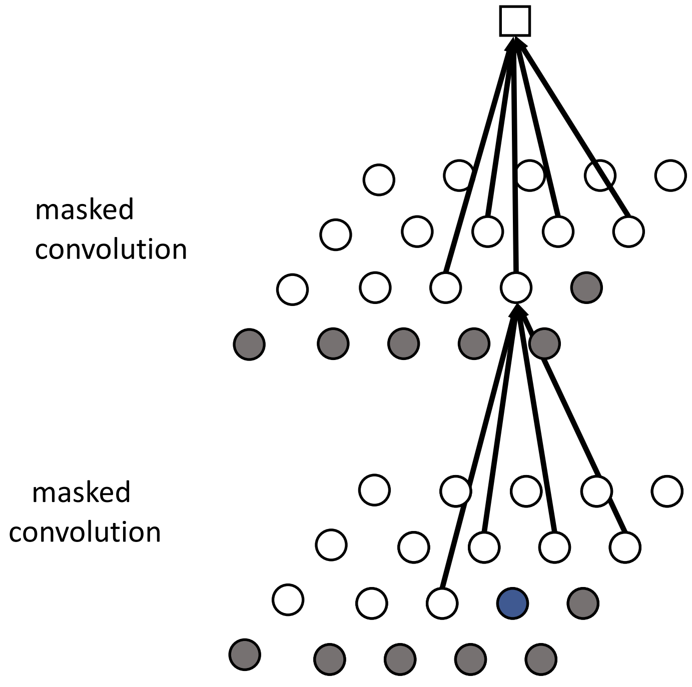

Diagonal BiLSTM

- Using CNN and RNN for modeling $p(x_k|\boldsymbol{x}_{<k})$ [Oord et al., 2016]
  - Pixel CNN use masked convolutional layer (for $\boldsymbol{x}_{>k}$)
  - Row LSTM use LSTMs, generating image row-by-row (not pixel-by-pixel)
  - Diagonal BiLSTM use bi-directional LSTMs, to generate image pixel-by-pixel

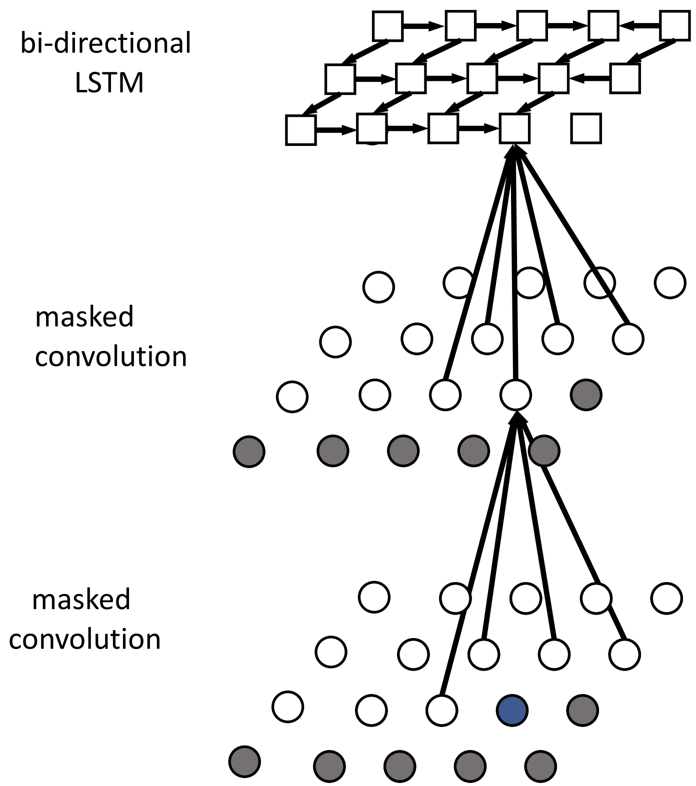

Diagonal BiLSTM

Pixel Convolutional/Recurrent Neural Network (PixelCNN/PixelRNN)

- Using CNN and RNN for modeling $p(x_k|\boldsymbol{x}_{<k})$ [Oord et al., 2016]
  - Pixel CNN use masked convolutional layer (for $\boldsymbol{x}_{>k}$)
  - Row LSTM use LSTMs, generating image row-by-row (not pixel-by-pixel)
  - Diagonal BiLSTM use bi-directional LSTMs, to generate image pixel-by-pixel

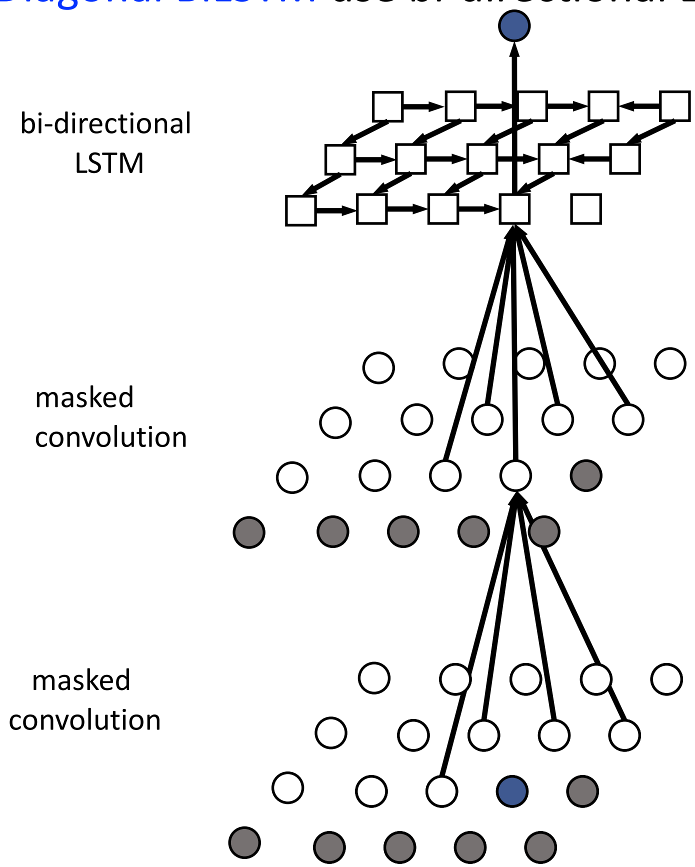

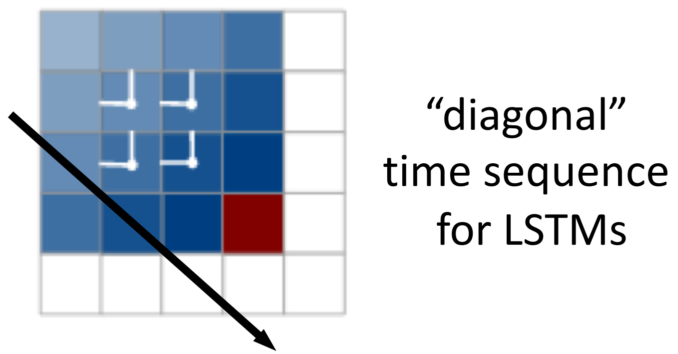

Diagonal BiLSTM

- Using CNN and RNN for modeling $p(x_k|\boldsymbol{x}_{<k})$ [Oord et al., 2016]
  - Pixel CNN use masked convolutional layer (for $\boldsymbol{x}_{>k}$)
  - Row LSTM use LSTMs, generating image row-by-row (not pixel-by-pixel)
  - Diagonal BiLSTM use bi-directional LSTMs, to generate image pixel-by-pixel

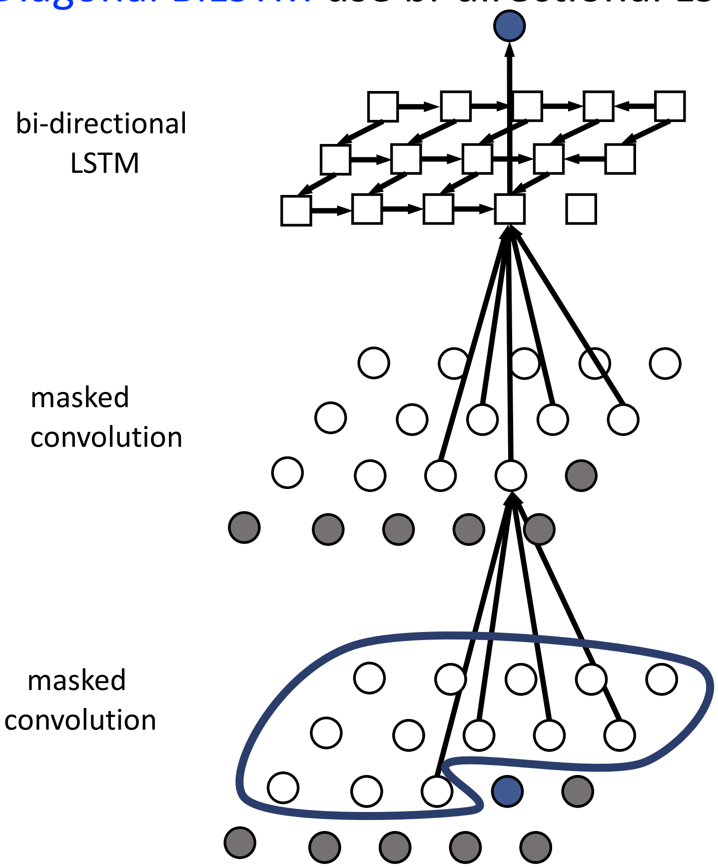

Diagonal BiLSTM

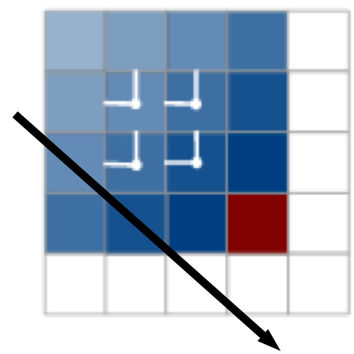

"diagonal" time sequence for LSTMs

- Receptive field now covers every pixels generated previously

- Image generation results from CIFAR-10 and ImageNet:

CIFAR-10

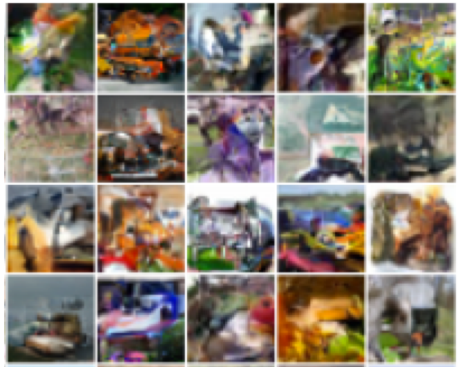

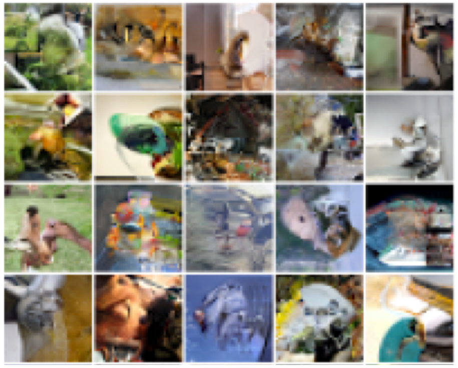

ImageNet

- Evaluation of negative log-likelihood (NLL) on MNIST and CIFAR-10 dataset:

Only explicit models (not GAN) can compute NLL

Model	NLL Test
PixelCNN:	81.30
Row LSTM:	80.54
Diagonal BiLSTM (1 layer, $h = 32$):	**80.75**
Diagonal BiLSTM (7 layers, $h = 16$):	**79.20**

MNIST

Model	NLL Test (Train)
PixelCNN:	3.14 (3.08)
Row LSTM:	3.07 (3.00)
Diagonal BiLSTM:	**3.00** (2.93)

CIFAR-10

- PixelCNN is easiest to train and Diagonal BiLSTM performs best

- Modifying data distribution by flow (sequence) of invertible transformations:

$$\boldsymbol{x} = \boldsymbol{z}_0 \;\rightarrow\; \boldsymbol{z}_T = f_T \circ f_{T-1} \circ \cdots f_1(\boldsymbol{z}_0) \qquad \boldsymbol{z}_t \in \mathbb{R}^K$$

  - Final variable follows some specified prior $p_T(\boldsymbol{z}_T)$

- Data distribution is explicitly modeled by change-of-variables formula:

$$\log p(\boldsymbol{x}) = \log p(\boldsymbol{z}_0) = \log p_T(\boldsymbol{z}_T) + \sum_{t=1}^{T} \log \left| \det \left(\frac{\partial f_t(\boldsymbol{z}_{t-1})}{\partial \boldsymbol{z}_{t-1}} \right) \right|$$

  - Log-likelihood $\log p(\boldsymbol{x})$ can be maximized directly

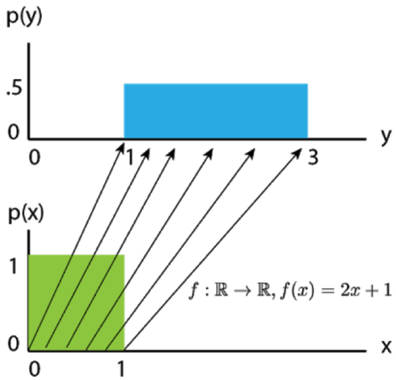

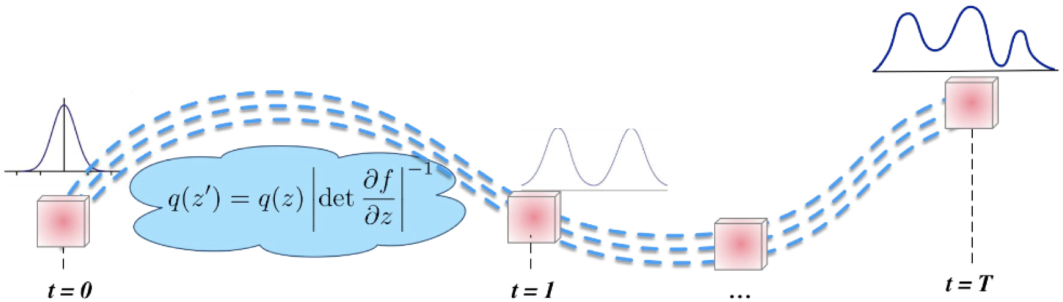

* source: Jang, https://blog.evjang.com/2018/01/nf1.html,
Mohamed et al., https://www.shakirm.com/slides/DeepGenModelsTutorial.pdf

Flow-based Models

- Modifying data distribution by flow (sequence) of invertible transformations:

$$\boldsymbol{x} = \boldsymbol{z}_0 \quad \boldsymbol{\rightarrow} \quad \boldsymbol{z}_T = f_T \circ f_{T-1} \circ \cdots f_1(\boldsymbol{z}_0) \qquad\qquad \boldsymbol{z}_t \in \mathbb{R}^K$$

  - Final variable follows some specified prior $p_T(\boldsymbol{z}_T)$

- Data distribution is explicitly modeled by change-of-variables formula:

$$\log p(\boldsymbol{x}) = \log p(\boldsymbol{z}_0) = \log p_T(\boldsymbol{z}_T) + \sum_{t=1}^{T} \log \left| \det \left(\frac{\partial f_t(\boldsymbol{z}_{t-1})}{\partial \boldsymbol{z}_{t-1}} \right) \right|$$

  - Log-likelihood $\log p(\boldsymbol{x})$ can be maximized directly
  - Naïvely computing $\log \left|\det\left(\partial f_t(\boldsymbol{z}_{t-1}) / \partial \boldsymbol{z}_{t-1}\right)\right|$ requires $\mathcal{O}(K^3)$ complexity, which is not scalable for large-scale neural networks

How to design flexible yet tractable form of invertible transformations?

Design Schemes for Normalizing Flows

- To reduce complexity of log-det-Jacobian, prior works consider
  - Carefully designed architectures (low rank, coupling, autoregressive)
  - Stochastic estimator of free-form Jacobian

1. Det Identities

Planar NF
Sylvester NF
...

Jacobian

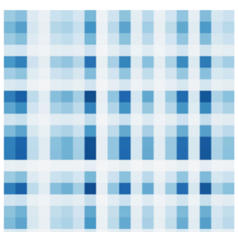

(Low rank)

2. Coupling Blocks

NICE
Real NVP
Glow
...

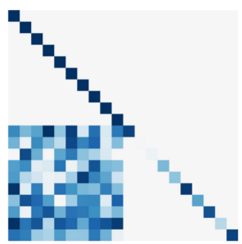

(Lower triangular + structured)

3. Autoregressive

Inverse AF
Neural AF
Masked AF
...

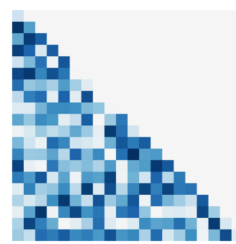

(Lower triangular)

4. Unbiased Estimation

FFJORD
Residual Flows

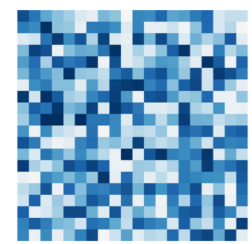

(Arbitrary)

* source: Chen, https://www.cs.toronto.edu/~duvenaud/talks/residual_flows_slides.pdf

- To reduce complexity of log-det-Jacobian, prior works consider
  - Carefully designed architectures (low rank, coupling, autoregressive)
  - Stochastic estimator of free-form Jacobian

1. Det Identities

Planar NF
Sylvester NF
...

Jacobian

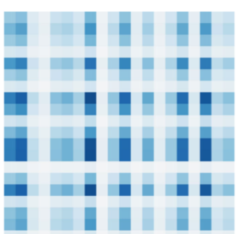

(Low rank)

* source: Chen, https://www.cs.toronto.edu/~duvenaud/talks/residual_flows_slides.pdf

- Basic layers with linear log-det-Jacobian complexity [Rezende et al., 2015]

- Planar flow: $f(\mathbf{z}) = \mathbf{z} + \mathbf{u}h(\mathbf{w}^\intercal \mathbf{z} + b)$
  - Determinant of Jacobian is $\left|\det \frac{\partial f}{\partial \mathbf{z}}\right| = |1 + \mathbf{u}^\intercal h'(\mathbf{w}^\intercal \mathbf{z} + b)\mathbf{w}|$

- Radial flow: $f(\mathbf{z}) = \mathbf{z} + \beta h(\alpha, r)(\mathbf{z} - \mathbf{z}_0)$ $(r = |\mathbf{z} - \mathbf{z}_0|,\ h(\alpha, r) = 1/(\alpha + r))$
  - Determinant of Jacobian is $[1 + \beta h(\alpha, r)]^{d-1}[1 + \beta h(\alpha, r) + h'(\alpha, r)r)]$

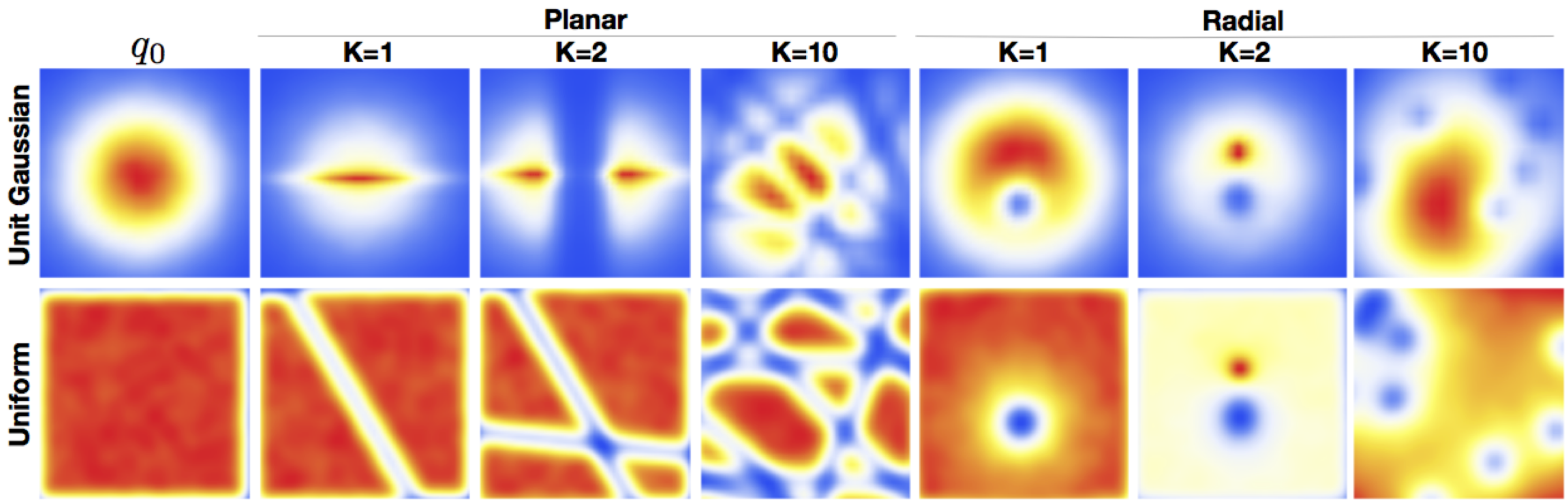

- To reduce complexity of log-det-Jacobian, prior works consider
  - Carefully designed architectures (low rank, coupling, autoregressive)
  - Stochastic estimator of free-form Jacobian

2. Coupling Blocks

NICE
Real NVP
Glow
...

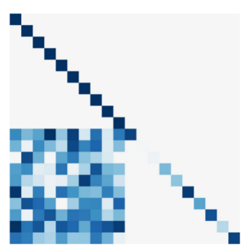

(Lower triangular + structured)

* source: Chen, https://www.cs.toronto.edu/~duvenaud/talks/residual_flows_slides.pdf

- Coupling layer $\boldsymbol{z}_t = f_t(\boldsymbol{z}_{t-1})$ for flow with tractable inference [Dinh et al., 2017]:
  1. Partition the variable into two parts:

$$\boldsymbol{z}_{t-1} \rightarrow [\boldsymbol{z}_{t-1,1:d}, \boldsymbol{z}_{t-1,d+1:K}]$$

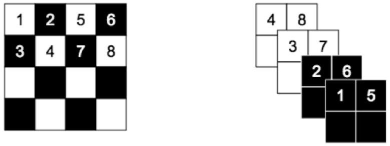

spatial-partition channel-partition

  2. Coupling law defines a simple invertible transformation of the first partition given the second partition (g and m are described later)

$$\boldsymbol{z}_{t,d+1:K} = g(\boldsymbol{z}_{t-1,d+1:K}; m(\boldsymbol{z}_{t-1,1:d}))$$

  3. Second partition is left invariant ($\boldsymbol{z}_{t,1:d} = \boldsymbol{z}_{t-1,1:d}$)

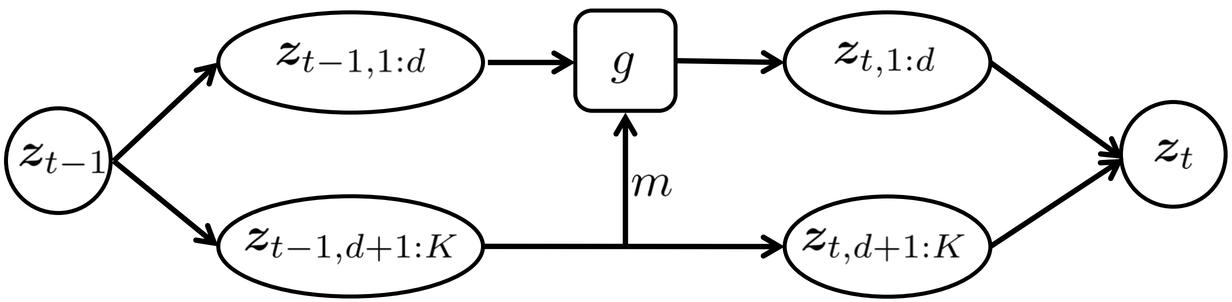

- Affine coupling layer was shown to be effective in practice:

$$\begin{aligned}\boldsymbol{z}_{t,d+1:K} &= g(\boldsymbol{z}_{t-1,d+1:K}; m(\boldsymbol{z}_{t-1,1:d})) \\ &= \boldsymbol{z}_{t-1,d+1:K} \odot \exp(m_1(\boldsymbol{z}_{t-1,1:d})) + m_2(\boldsymbol{z}_{t-1,1:d})\end{aligned}$$

element-wise product

neural networks

- Jacobian of each transformation becomes a lower triangular matrix:

$$\frac{\partial f_{t-1}(\boldsymbol{z}_{t-1})}{\partial \boldsymbol{z}_{t-1}} = \begin{bmatrix} \mathbb{I} & \mathbf{0} \\ \frac{\partial g_{t-1}(\boldsymbol{z}_{t-1})}{\partial \boldsymbol{z}_{t-1}} & \operatorname{diag}(\exp(m_1(\boldsymbol{z}_{t-1,1:d}))) \end{bmatrix} \rightarrow \begin{bmatrix} a_{11} & 0 & \cdots & 0 \\ & a_{22} & 0 & \vdots \\ & & \ddots & 0 \\ & & & a_{KK} \end{bmatrix}$$

- Inference for such transformations can be done in tractable time
  - Determinant of lower triangular matrix is a product of diagonals

$$\log p(\boldsymbol{x}) = \log p(\boldsymbol{z}_0) = \log p_T(\boldsymbol{z}_T) + \sum_{t=1}^{T} \log \left| \det \left(\frac{\partial f_t(\boldsymbol{z}_{t-1})}{\partial \boldsymbol{z}_{t-1}} \right) \right|$$

- For each coupling layer, there exists asymmetry since the first partition $z_{t-1,1:d}$ is left invariant
  - Two coupling layers are paired alternatively to overcome this issue

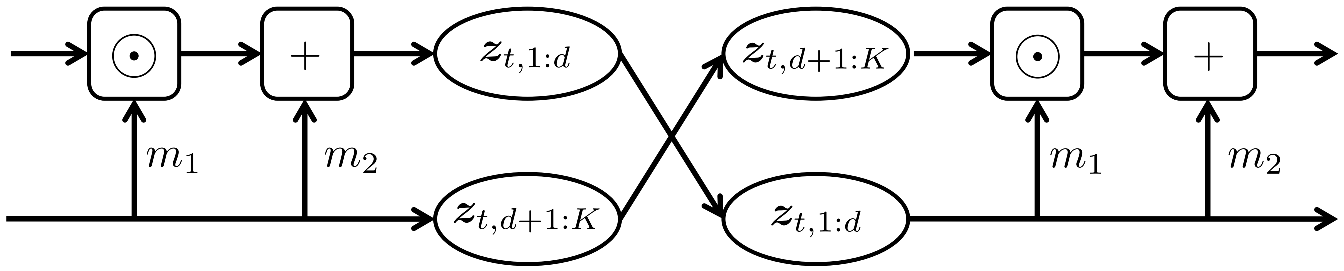

- Multi-scale architectures are used
  - Half variables follow Gaussian distribution at each scale

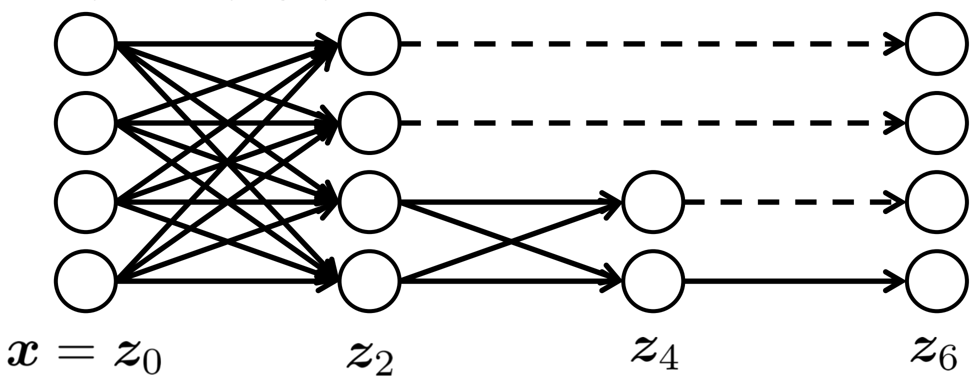

$$p(z_3) = \mathcal{N}(z_3; \mathbf{0}, \mathbf{1})$$

Design Schemes for Normalizing Flows

- To reduce complexity of log-det-Jacobian, prior works consider
  - Carefully designed architectures (low rank, coupling, autoregressive)
  - Stochastic estimator of free-form Jacobian

3. Autoregressive

Inverse AF
Neural AF
Masked AF
...

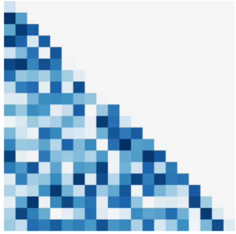

(Lower triangular)

* source: Chen, https://www.cs.toronto.edu/~duvenaud/talks/residual_flows_slides.pdf

- Inverse autoregressive flow (IAF) modifies each dimension of variable in autoregressive manner [Kingma et al., 2016]:
  - Forward pass $z_0 \to z_T$ is fast, but backward pass $z_T \to z_0$ is slow
    - Used for VAE posterior: Only forward pass is required for approx. posterior

$$\boldsymbol{z}_{t,d} = \mu_{t,d}(\boldsymbol{z}_{t-1,1:d-1}) + \sigma_{t,d}(\boldsymbol{z}_{t-1,1:d-1})\boldsymbol{z}_{t-1,d}$$

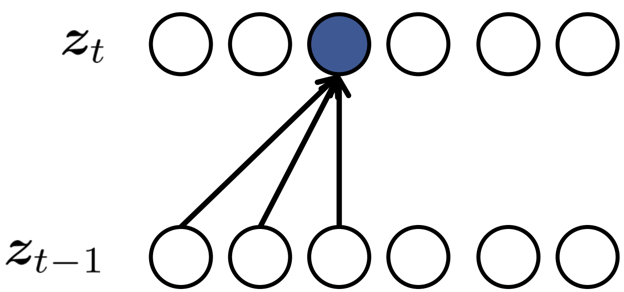

case of $d = 3$

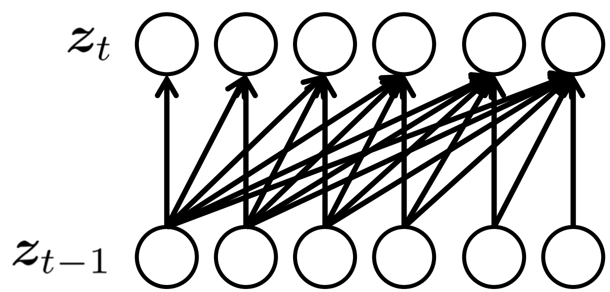

updates done in parallel

  - Inference for corresponding normalizing flow is efficient:

$$\log q(\boldsymbol{z}|\boldsymbol{x}) = \log q_0(\boldsymbol{z}_0|\boldsymbol{x}) + \sum_{t=1}^{T} \log \left| \det \left(\frac{\partial f_t(\boldsymbol{z}_{t-1})}{\partial \boldsymbol{z}_{t-1}} \right) \right|$$

$$\begin{bmatrix} \sigma_{t,1} & 0 & \cdots & 0 \\ & \sigma_{t,2} & 0 & \vdots \\ & & \ddots & 0 \\ & & & \sigma_{t,K} \end{bmatrix}$$

- To reduce complexity of log-det-Jacobian, prior works consider
  - Carefully designed architectures (low rank, coupling, autoregressive)
  - Stochastic estimator of free-form Jacobian

4. Unbiased Estimation

FFJORD
Residual Flows

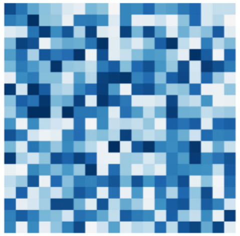

(Arbitrary)

* source: Chen, https://www.cs.toronto.edu/~duvenaud/talks/residual_flows_slides.pdf

Continuous Normalizing Flow (CNF)

- Discrete normalizing flows need a carefully designed (less expressive) layers to achieve affordable (not cubic) complexity
  → Continuous normalizing flow affords an arbitrary network architecture

- Consider a continuous transformation $\frac{d\mathbf{z}}{dt} = f(\mathbf{z}(t), t)$ (instead of $\mathbf{z}_1 = f(\mathbf{z}_0)$), then the sampling can be done by an **ordinary differential equation (ODE)**:

$$z(t_1) = z(t_0) + \int_{t_0}^{t_1} f(z(t), t, \theta) dt$$

  - Here, the change in log-probability also follows an ODE:

$$\log p(\mathbf{z}(t_1)) = \log p(\mathbf{z}(t_0)) - \int_{t_0}^{t_1} \mathrm{Tr}\left(\frac{\partial f}{\partial \mathrm{z}(t)}\right) dt$$

  - **Remark:** We only need a **trace** (not a **determinant**) to compute likelihood

  - The network $f(z(t), t, \theta)$ is learned by gradient descent (backpropagation follows another ODE) [Chen et al., 20018; Grathwohl et al., 2019]

References (VAE)

[Kingma et al., 2013] Auto-Encoding Variational Bayes, ICLR 2013
link: https://arxiv.org/abs/1802.06455

[Burda et al., 2016] Importance Weighted Autoencoders, ICLR 2016
link: https://arxiv.org/abs/1509.00519

[Kim et al., 2018] Semi-Amortized Variational Autoencoders, ICML 2018
link: https://arxiv.org/abs/1802.02550

[Bowman et al., 2016] Generating Sentences from a Continuous Space, CONLL 2016
link: https://arxiv.org/abs/1511.06349

[Razavi et al., 2019a] Preventing Posterior Collapse with delta-VAEs, ICLR 2019
link: https://arxiv.org/abs/1901.03416

[Tolstikhin et al., 2018] Wasserstein Auto-Encoders, ICLR 2018
link: https://arxiv.org/abs/1711.01558

[He et al., 2019] Lagging Inference Networks and Posterior Collapse in Variational Autoencoders, ICLR 2019
link: https://arxiv.org/abs/1901.05534

[Oord et al., 2017] Neural Discrete Representation Learning, NeurIPS 2017
link: https://arxiv.org/abs/1711.00937

[Razavi et al., 2017b] Generating Diverse High-Fidelity Images with VQ-VAE-2, NeurIPS 2019
link: https://arxiv.org/abs/1906.00446

[Vahdat et al., 2020] NVAE: A Deep Hierarchical Variational Autoencoder, NeurIPS 2020
link: https://arxiv.org/abs/2007.03898

[Sohl-Dickstein et al., 2015] Deep Unsupervised Learning using Nonequilibrium Thermodynamics, ICML 2015
link: https://arxiv.org/abs/1503.03585

[Ho et al., 2020] Denoising Diffusion Probabilistic Models, NeurIPS 2020
link: https://arxiv.org/abs/2006.11239

References (EBM, score matching)

[LeCun et al., 2006] A Tutorial on Energy-Based Learning, Technical report 2006
link: http://yann.lecun.com/exdb/publis/pdf/lecun-06.pdf

[Du & Mordatch, 2019] Implicit Generation and Generalization in Energy-Based Models, NeurIPS 2019
link: https://arxiv.org/abs/1903.08689

[Welling & Teh, 2011] Bayesian Learning via Stochastic Gradient Langevin Dynamics, ICML 2011
link: https://dl.acm.org/doi/10.5555/3104482.3104568

[Zhao et al., 2017] Energy-based Generative Adversarial Network, ICLR 2017
link: https://arxiv.org/abs/1609.03126

[Grathwohl et al., 2020] Your Classifier is Secretly an Energy Based Model and You Should Treat it Like One, ICLR 2020
link: https://arxiv.org/abs/1912.03263

[Song & Kingma, 2021] How to Train Your Energy-Based Models, arXiv 2021
link: https://arxiv.org/abs/2101.03288

[Hyvärinen, 2005] Estimation of Non-Normalized Statistical Models by Score Matching, JMLR 2005
link: https://jmlr.org/papers/v6/hyvarinen05a.html

[Vincent, 2011] A Connection Between Score Matching and Denoising Autoencoders, Neural Computation 2011
link: https://ieeexplore.ieee.org/document/6795935

[Song et al., 2019] Generative Modeling by Estimating Gradients of the Data Distribution, NeurIPS 2019
link: https://arxiv.org/abs/1907.05600

[Song et al., 2021] Score-Based Generative Modeling through Stochastic Differential Equations, ICLR 2021
link: https://arxiv.org/abs/2011.13456

References (AR, flow)

[Oord et al., 2016] Pixel Recurrent Neural Networks, ICML 2016
link: https://arxiv.org/abs/1601.06759

[Oord et al., 2017] WaveNet: A Generative Model for Raw Audio, arXiv 2017
link: https://arxiv.org/abs/1703.01961

[Rezende et al., 2015] Variational Inference with Normalizing Flows, ICML 2015
link: https://arxiv.org/abs/1705.08665

[Dinh et al., 2017] Density Estimation using Real NVP, ICLR 2017
link: https://arxiv.org/abs/1605.08803

[Kingma et al., 2018] Generative Flow with Invertible 1x1 Convolutions, NeurIPS 2018
link: https://arxiv.org/abs/1807.03039

[Kingma et al., 2016] Improving Inference with Inverse Autoregressive Flows, NeurIPS 2016
link: https://arxiv.org/abs/1710.10628

[Chen et al., 2018] Neural Ordinary Differential Equations, NeurIPS 2018
link: https://arxiv.org/abs/1806.07366

[Grathwohl et al., 2019] FFJORD: Free-Form Continuous Dynamics for Scalable Reversible Generative Models, ICLR 2019
link: https://arxiv.org/abs/1810.01367

[Chen et al., 2019] Residual Flows for Invertible Generative Modeling, NeurIPS 2019
link: https://arxiv.org/abs/1906.02735